THE EFFECT OF OXYGEN ON THE ULTRAVIOLET OPTICAL ABSORPTION BANDS OF MAGNESIUM OXIDE

by

DEWI GORDON EVANS

A THESIS SUBMITTED IN PARTIAL FULFILMENT

OF THE REQUIREMENTS FOR THE DEGREE OF

MASTER OF APPLIED SCIENCE

IN THE DEPARTMENT

OF

MINING AND METALLURGY

We accept this thesis as conforming to the

standard required from candidates for

the degree of MASTER OF APPLIED SCIENCE

Members of the Department of Mining and Metallurgy

THE UNIVERSITY OF BRITISH COLUMBIA

March, 1961

In presenting this thesis in partial fulfilment of the requirements for an advanced degree at the University of British Columbia, I agree that the Library shall make it freely available for reference and study. I further agree that permission for extensive copying of this thesis for scholarly purposes may be granted by the Head of my Department or by his representatives. It is understood that copying or publication of this thesis for financial gain shall not be allowed without my written permission.

Department of Mining and Metallurgy

The University of British Columbia,
Vancouver 8, Canada.

Date March 30, 1961

ABSTRACT

An investigation into the effect of oxygen on the three ultraviolet optical absorption bands in magnesium oxide was carried out. These peaks were located at 5.75, 5.0 and 4.40 eV within the range 212 to 350 mμ.

The single crystal platelets were heated in air or oxygen for increasing times at various temperatures. It was found that the increase in peak height with time followed a diffusion relation.

A mechanism of formation of the centers causing the 5.75 and 4.40 eV peaks was proposed. The mechanism was based on the oxidation of iron and manganese impurities and the diffusion of magnesium to the crystal surface. The absorbing center was defined as $(Fe^{+3}. V_{Mg}^{+2})$. From this it was shown that the diffusion process governing both the 5.75 and the 4.40 eV peaks followed the same Arrhenius relation:

$$D = 1.7 \times 10^{5} e^{\frac{-77,000}{RT}} \text{ cm}^2/\text{sec.}$$

over the temperature range of 800 to 1100° C.

No similar conclusions could be drawn concerning the 5.0 eV peak.

ACKNOWLEDGEMENT

The author wishes to thank Professor W. M. Armstrong and Dr. A. C. D. Chaklader for their direction, encouragement and enthusiasm throughout this investigation. Indebtedness is also acknowledged to Mr. R. G. Butters for his fine technical assistance and to (Mrs.) A. M. Armstrong for her enlightening discussionsand helpful suggestions.

This project was financed by the Defence Research Board through Research Grant 7510-32 and by the National Research Council of Canada.

TABLE OF CONTENTS

TABLE OF CONTENTS (continued)

LIST OF FIGURES

TABLES

APPENDICES

THE EFFECT OF OXYGEN ON THE ULTRAVIOLET OPTICAL ABSORPTION BANDS OF MAGNESIUM OXIDE

I. INTRODUCTION

A. General

Recent interest in ceramics as components of engineering materials such as ceramic-coated parts and cermets has resulted in this department initiating a programme directed toward the accumulation of fundamental knowledge of the bond and bonding mechanisms between metals and ceramics[25,26,27]. One of the main factors in obtaining a good metal-ceramic bond is the magnitude of the surface energies involved and the effect of surface active impurities and alloying elements on these energies. Clarke[27], using the sessile-drop method, investigated the effect of alloying elements in the liquid-metal drop on the liquid-solid interfacial energy. He found that small alloying additions produced significant energy changes. Both Clarke and Hasselman[26] found evidence of interdiffusion of the alloying and bulk elements across the interface between the metal and the ceramic. Therefore, a knowledge of the defect structure, impurity content and the behaviour of the ceramic component under various conditions would be a desirable addition to the knowledge so far acquired. An investigation into the coloring of magnesium oxide by X-rays and by oxygen appeared to be a good basis for an investigation of this kind.

B. Summary of Previous Work

A well-known phenomenon associated with alkali halide crystals is their ability to be "coloured" by high energy beams (X-rays, ultra-violet light, electrons, neutrons, etc.) or by introducing into the crystals an excess of either component[1,2]. In addition, recent investigations have found coloration effects due to the introduction of impurities. This coloring process may be detected by the presence of one or more peaks or

bands in the optical absorption spectrum of the crystals. Each band is characteristic of a color center which generally consists of positive or negative vacancies, singly or in groups, upon which electrons or holes may be trapped.

Similar investigations into the coloration of magnesium oxide produced similar results. A deep purple coloration was produced by ultraviolet irradiation[3]; further experimentation[4] showed that this coloration could also be introduced by X-rays with accompanying optical absorption peaks near 2.3, 4.4 and 5.6 eV. Weber[5] examined the effect of an excess of either component as well as of X-rays on these bands with the following results:

1) MgO crystals could be additively colored by both oxygen and magnesium vapour. Oxygen addition produced peaks at 4.3 and 5.7 eV; Mg vapour produced peaks near 2.4, 3.6 and 5.0 eV.

2) The rate of increase in height of the ultraviolet absorption bands when the crystal was heated in oxygen was governed by a diffusion mechanism.

3) The amount of oxygen coloration reached a limiting or saturation value; the saturation level increased linearly with the logarithm of the oxygen pressure.

4) The X-ray induced spectrum could be depicted as a superposition of the oxygen and magnesium bands.

5) The X-ray induced spectrum could be completely removed by warming and the oxygen induced spectrum by vacuum annealing.

6) One of the more important processes in the oxygen diffusion was the adsorption of oxygen on the inner surfaces of the crystal; however, not all the oxygen present was optically detected.

Recently considerable interest has been displayed in MgO especially since large single crystals have become available. Experiments have been conducted on the defect structure and electronic properties of MgO using the Hall effect[6], photoconductivity[7,8] post bombardment conductivity[9,10], X-ray and ultraviolet coloring[11,12,13,14], reflectivity[15], high temperature conductivity[6], luminescence[16,17] and electron spin resonance[17,18,19,20,21]. Perhaps the most extensive investigation of the optical and electrical properties of MgO was carried out by Shepherd and his associates[22].

Most of the investigations have been concerned with the so-called "oxygen-bands" at 4.4 and at 5.7 eV, and appear to be directed toward the construction of a band model for MgO as well as defining the nature of the defects causing the localized transitions. The energy gap between the conduction and valence bands has been estimated by Johnson[14], using ultraviolet excitation and optical methods; Yamashita[11], using X-rays and the tight binding approximation; and Reilling and Hensley[15], using reflectivity measurements. Johnson estimated $\geq$7.4 eV for the energy gap, Yamashita 7.6 eV, and Reilling and Hensley, 8.7 eV.

Attempts at defining the nature of the defects causing transitions to and from localized states have not been without controversy. Day[7] found photoconductivity peaks at 1.2, 2.1, 3.7 and 4.8 eV; the latter three agreed with optical absorption peaks for Mg-excess crystals observed by Weber[5]. Day concluded that holes rather than electrons produced the photoconduction since a narrow excited region of a crystal between two electrodes which was irradiated by 4.0 eV light and subsequently scanned by longer wavelength light always moved toward the negative electrode under application of an

electric field. Evidently the results of two other investigations[6,23] substantiated Day's postulate. However, Peria[8,22] attributed the bands at 3.6 and 4.8 eV to the strong optical absorption maximum near 4.4 eV and a minimum near 4.8 eV. A photoconductivity spectrum uncorrected for this absorption effect would therefore lead to the two peaks observed by Day. Moreover, through his method of analysis Peria obtained two photoconductivity peaks of Gaussian shape located at 4.05 and 5.05 eV. Peria attributed the low energy peak to hole transitions and the 5.05 eV peak to electron transitions.

Although the results obtained from the coloring studies on MgO were similar to those obtained for the alkali halides, it was recognized that impurities (principally those of variable valence) were probably the dominant factor in producing the optical bands. This inferred that there were no optically detectable color centers analogous to those in the alkali halides. Indeed, Wertz, et al [18] defined the F-center from electron spin resonance (E.S.R.) studies as an oxygen vacancy between two Mg^{25} ions; no detectable amounts of this center could be produced by the same treatments used to produce color-centers in the alkali halides.

Johnson[14] extended optical absorption measurement to the vacuum ultraviolet. He observed two additional "oxygen excess" peaks at 6.2 and 6.7 eV; only below 1700 Å was the optical absorption impurity independent. The work of Wertz, et al [18,19], Haxby[22], Peria[8,22], and Hansler and Segelken[17] verified the nature of the impurity dependence of the observed optical absorption, luminescence and photoconductivity phenomena. Clarke[13], however, concluded that only the 6.7 eV band could be ascribed to impurities. All the other bands were attributed to magnesium or oxygen vacancies in their

neutral states or with trapped electrons or holes (analogous to alkali halide centers).

Haxby[22] has shown that both Mn and Fe impurities affect the excess oxygen bands, iron having by far the dominant effect. He found that the saturation level of the 4.4 eV band increased approximately linearly with increasing iron and manganese contents. Moreover, extrapolation of the iron line to zero concentration resulted in zero absorption at 4.4 eV; that is, no bands at 4.4 or 5.7 eV would be observed at zero iron (and manganese) content. Crystals heavily "doped" with cobalt and chromium, however, exhibited entirely different behaviour. These two impurities appeared to mask the 5.7 eV peak but the 4.4 eV peak was unaffected by the impurity additions. Furthermore, vacuum annealing was only partially effective in removing the ultraviolet absorption. (This agreed well with the observations of Hansler and Segelken[17] on chromium-doped crystals). Under oxygen treatment the chromium-doped crystals have first a decreasing ultraviolet absorption with time and then an increasing absorption. The spectrum of the increase showed little resemblance to the iron-in-MgO spectrum. Haxby also found that the saturation level for the iron (plus manganese) spectrum decreased with increasing temperature.

Further examination of the X-ray induced coloring by Wertz, et al [18] established that Fe^{+3} with an associated magnesium vacancy and a trapped hole was probably the center responsible for the oxygen bands. This postulate fitted some of the results of Peria[8] and the X-ray work of Soshea, et al [12]. It was also observed by Wertz, et al that under X-irradiation the intensity of the Cr^{+3} E.S.R. peak decreased while the Fe^{+3} peak increased. On decay the reverse was observed. This indicated

that reactions of the type:

$$Fe^{+2} \rightarrow Fe^{+3} + 1\,e$$

$$Cr^{+3} + 1\,e \rightarrow Cr^{+2}$$

might be taking place under X-irradiation. Haxby has interpreted these reactions and others involving electrons, holes, and positive and negative vacancies using the method of Kröger and Vink[24].

Low[20,21] found absorption peaks near 2.0, 2.8 and 3.65 eV for Cr^{+3} doped MgO crystals (which agreed with Haxby's observations) and no appreciable absorption due to Mn^{+2}. Low found no vacancies associated with the Cr^{+3} ion; in contrast, Wertz and Auzins[19] assumed at least one Mg^{+2} vacancy for every two Cr^{+3} ions. Hansler and Segelken[17] used Cr_2O_3-doped crystals to produce Cr^{+2} and Cr^{+3} spectra. They found an additional Cr^{+3} peak at 5.9 eV and a Cr^{+2} peak at 5.0 eV. These and other data obtained from luminescence studies enabled them to formulate the valence changes of iron and chromium into a band scheme.

Soshea, et al [12] used primarily X-ray induced spectra to show by means of a mathematical analysis that a third ultraviolet peak occurred near 4.8 eV. This peak was found by Haxby to be evident also in oxygen-treated crystals. Weber[5] obtained some evidence of a peak near 5.0 eV when the X-ray induced spectrum was measured at low temperatures. The peak was evident without analysis. Soshea, et al took issue with a Mg-excess peak near 4.8 eV found by Weber, stating that the 4.8 eV band was spurious and that the true spectrum was the difference between two Mg-excess crystals rather than the difference before and after Mg coloration.

This brief summary indicates that the results of previous workers on the coloring of magnesium oxide by various means tend to

favour the following conclusions:

1) The type and process of coloring appears to depend on the amount and species of variable valence impurities contained in the crystals. Therefore there are probably no optically detectable color centers in MgO analogous to those found in the alkali halides.

2) The same "oxygen excess" bands in the ultraviolet region can be produced by high energy irradiation as well as by heating the crystals in the presence of oxygen. Possibly these bands are caused by the valence change of Fe^{+2} to Fe^{+3} (and Mn^{+2} to Mn^{+3}) and occur near 4.4, 4.9 and 5.7 eV. The only difference between the two treatments was that the irradiation-induced spectrum was unstable whereas the oxygen induced absorption was stable indefinitely.

3) The amount of ultraviolet optical absorption introduced with time by the oxygen heat treatment is governed by adsorption and diffusion mechanisms.

C. Scope of Present Investigation

This project was primarily concerned with the diffusion mechanism observed by Weber[5] and later by Shepherd[26] when magnesium oxide was heated in oxygen. The data and results were obtained through optical absorption measurements on the three ultraviolet peaks; the method used in interpretation of the results was similar to that of Moulson and Roberts[28]. No attempt was made to correlate the changes in the magnesium oxide defect structure or the amount and type of impurity present to any surface energy changes that may have resulted through the oxygen treatment.

II. EXPERIMENTAL

A. Material

The magnesium oxide was supplied by the Norton Company as Optical Grade Magnorite. This consisted of random sized pieces, each composed of one or more large single crystals. The color of the crystals ranged from colorless and transparent through yellow to opaque orange. Apparently the color depended on the impurity content (in this case iron; the color imparted by appreciable amounts of chromium is green[20,21]). Sample analyses performed by J. H. Kelly of The Steel Company of Canada (see Appendix A), are shown in Table I.

TABLE I

Analyses of MgO Crystals

Crystal	Color	Composition (wt. %)						
		Al	Mn	Fe	Si	Cu	Cr	Ca
Impure 1.	Opaque orange	0.024	0.0007	0.042	0.015	0.0013	0.009	0.011
2.		0.024	0.0027	0.036	0.030	0.0012	0.007	0.017
19 - 1.	Yellow transparent	0.007	0.0014	0.028	0.006	0.0005	0.005	0.005
2.		0.008	0.0016	0.028	0.010	0.0021	0.006	0.006
5 - 1.	Colorless transparent	0.034	0.0017	0.009	0.020	0.0013	0.006	0.006
2.		0.029	0.0014	0.013	0.018	0.0033	0.003	0.007
3.		0.022	0.0016	0.012	0.017	0.0020	0.005	0.005
4.		0.034	0.0016	0.008	0.018	0.0007	0.003	0.004
14 - 1.	Colorless transparent	0.022	0.0041	0.011	0.011	0.0005	0.008	0.008
2.		0.023	0.0041	0.005	0.007	0.0005	0.006	0.006
3.		0.010	0.0029	0.006	0.007	0.0011	0.007	0.005
4.		0.010	0.0018	0.007	0.006	0.0006	0.008	0.005

Only crystals 5 and 14 were used in the diffusion measurements.

B. Equipment

All the vacuum annealing of specimens was carried out in an induction furnace described elsewhere[26]. Standard resistance wound tube furnaces were used in the oxygen heat treating. These furnaces had a maximum operating temperature of 1100° C. and were regulated by a Wheelco temperature controller and a chromel-alumel thermocouple.

The optical absorption measurements were obtained using a Beckman Model DK Spectrophotometer. These measurements were mainly in the ultraviolet region from 212 to 350 mμ. Some readings were taken in the visible and the infra-red range up to 2800 mμ.

A special specimen holder (Figure 1.) was made to fit into the existing holder in the sample compartment of the Spectrophotometer. Although no X-ray work was performed during this project, the specimen holder was so constructed that crystals could also be colored by X-irradiation in the Norelco Fluorescence Analysis unit without removing the specimen. A sleeve could be slipped over the colored specimen to exclude visible light.

C. Experimental Procedures

The larger pieces of magnesium oxide were cleaved by means of a small hammer and chisel into smaller single crystal blocks. These blocks were further reduced by cleavage to platelets measuring approximately one-quarter to one-half inch square by twenty thousandths of an inch or less in thickness. The platelets were then vacuum annealed at 1200 to 1300° C. and 10^{-5} mm of Hg for 1½ hours or longer depending on thickness; this annealing removed any optical structure inherent in the as-received material.

Figure 1. Specimen Holder (center) with Specimen in Place, Balance of Apparatus for X-irradiation Work.

The platelets were chemically polished in hot phosphoric acid for 30 to 40 seconds. A mark was inscribed on one face of each specimen; this face received the incident light from the spectrophotometer and was exposed to the oxygen atmosphere to obtain unidirectional diffusion. The specimens were cleaned with either ethanol or acetone after which they were glued to the specimen holder with rubber cement and the vacuum annealed spectra taken. The specimens were cleaned before each subsequent optical absorption measurement.

Oxygen heat treatment of the magnesium oxide consisted of placing a specimen flat on another, larger crystal, putting this unit into an alumina boat and heating the specimen in a tube furnace for a specific time period, after which an optical absorption measurement was taken. A rough temperature setting on the controller was supplemented by temperature measurements before and after each run. Several readings were taken and the average temperature and fluctuation recorded. One thermocouple was used for all readings. After each optical measurement the boat and specimen were replaced in the same furnace position; the furnace temperature was taken at this point.

On removal the specimens were either allowed to cool in the boat or were effectively air-quenched by placing them quickly on the top of the furnace. The latter procedure when used for the higher temperature runs generally resulted in cracking of the specimen.

Two sets of data were obtained: one for heating in air (crystal 5) and one for heating in an essentially pure oxygen atmosphere (crystal 14). The oxygen atmosphere was achieved by flushing the furnace at a controlled rate. The effect of flow rate was checked (specimen 14 L).

Both the reproducibility of, and the effect of thickness on the growth rate of the ultraviolet absorption bands was also checked. This was accomplished using two specimens of different thicknesses (5 C 2 and 5 D 2) heated simultaneously at one temperature (1094° C.).

III. EXPERIMENTAL RESULTS AND OBSERVATIONS

A. Theory and Method of Analysing Data

1. Calculation of the Optical Absorption of the Centers

Transmission of monochromatic light through a transparent solid medium is governed by the relation[8]:

$$I = Io\,(1 - R)^2\, e^{-\mu l} \qquad \ldots\ldots (1)$$

where: Io = incident light intensity

I = transmitted light intensity

R = reflection coefficient

μ = linear absorption coefficient

l = light path length in the medium

Most of the data were obtained in terms of the optical density (d) where:

$$d = \log_{10} \frac{Io}{I} \qquad \ldots\ldots (2)$$

The combined optical density of a number of media is equivalent to the sum of the densities of the individual media[29]. This statement can also be applied to solutions:

1) Since the spectra of the MgO specimens in the vacuum annealed condition showed no structure (curve 1, Figure 2.) it was assumed that no absorbing species existed in the spectral region investigated. Therefore, for a particular wave length, the optical density in the vacuum annealed condition (d_M) ; that is, the optical density of the solvent, may be expressed by the equation:

$$d_M = -\log_{10} (1 - R)^2 + \frac{\mu}{2.3}\, l_M \qquad \ldots\ldots (3)$$

where: l_M = the crystal thickness

2) When the specimens were heated in the presence of oxygen the spectra contained peaks or bands (curve 2, Figure 2.) caused by the introduction of absorbing (defect) centers; that is, the solute. The overall density (d_A) may now be expressed as:

$$d_A = d_M + d_c \qquad \ldots\ldots (4)$$

where: d_c = optical density due to the defect centers alone

Assuming Beer's Law to hold for the centers then[29]:

$$d_c = \frac{\epsilon C}{2.3} l_c \qquad \ldots\ldots (5)$$

where: ϵ = molar absorption coefficient

C = concentration of absorbing species per unit volume

l_c = light path length in the absorbing centers

A further definition of C and l_c in equation (5) was necessary for the case of the absorbing species in MgO. Weber[5] showed that the concentration of centers versus distance from the crystal surface followed a parabolic diffusion profile. Therefore, the quantities l_c and C as measured optically were essentially average values and the product could be defined as:

$$C\, l_c = \int_{l=0}^{l=l \text{ at } C=0} C_l \, dl$$

where: l = distance from the crystal surface.

Furthermore, near the beginning of the heat treatment, $l_c < l_M$; when the specimen is completely saturated, $l_M = l_c$ assuming a homogeneous distribution of the absorbing species[28].

Equation (3) may be subtracted from (4) if:

i) the standard or reference (in this case air) is the same for both measurements,

ii) the dispersing and reflecting properties of the specimens do not change appreciably with treatment[8].

Therefore from (3) and (4):

$$d_A - d_M = \Delta d = d_c = \frac{\epsilon C}{2.3} l_c \qquad \ldots\ldots (6)$$

The quantity $\frac{\Delta d}{l_c}$ is then a measure of the concentration of absorbing species; ϵ is considered a constant, depending only on the nature of the absorbing species and the wavelength[30].

In determining Δd_t at time t the following procedure was used:

1. Using as an example specimen 14 J (Figure 2) heated 30 minutes in 1 atmosphere oxygen at 1084° C.:

   a) d_A at 282.5 (4.40 eV) = 0.469 (curve 2)

   b) correction to 100% transmission (T) due to the presence of the specimen holder (curve 3) = 0.937

   c) from (2):

$$d = \log_{10} \frac{Io}{I} = \log_{10} \frac{1}{T}$$

$$\therefore \quad \frac{1}{T} = \text{antilog } 0.469$$

$$\text{or} \quad T = 0.339$$

   d) corrected T = 0.937 (0.339) = 0.318

$$\therefore \text{ corrected } d_A = \log_{10} \frac{1}{0.318} = 0.498$$

   e) the same procedure was used to determine d_M from curve 1. This value deducted from d_A gives $\Delta d_t \times 10^3$ in Table II, Appendix B.

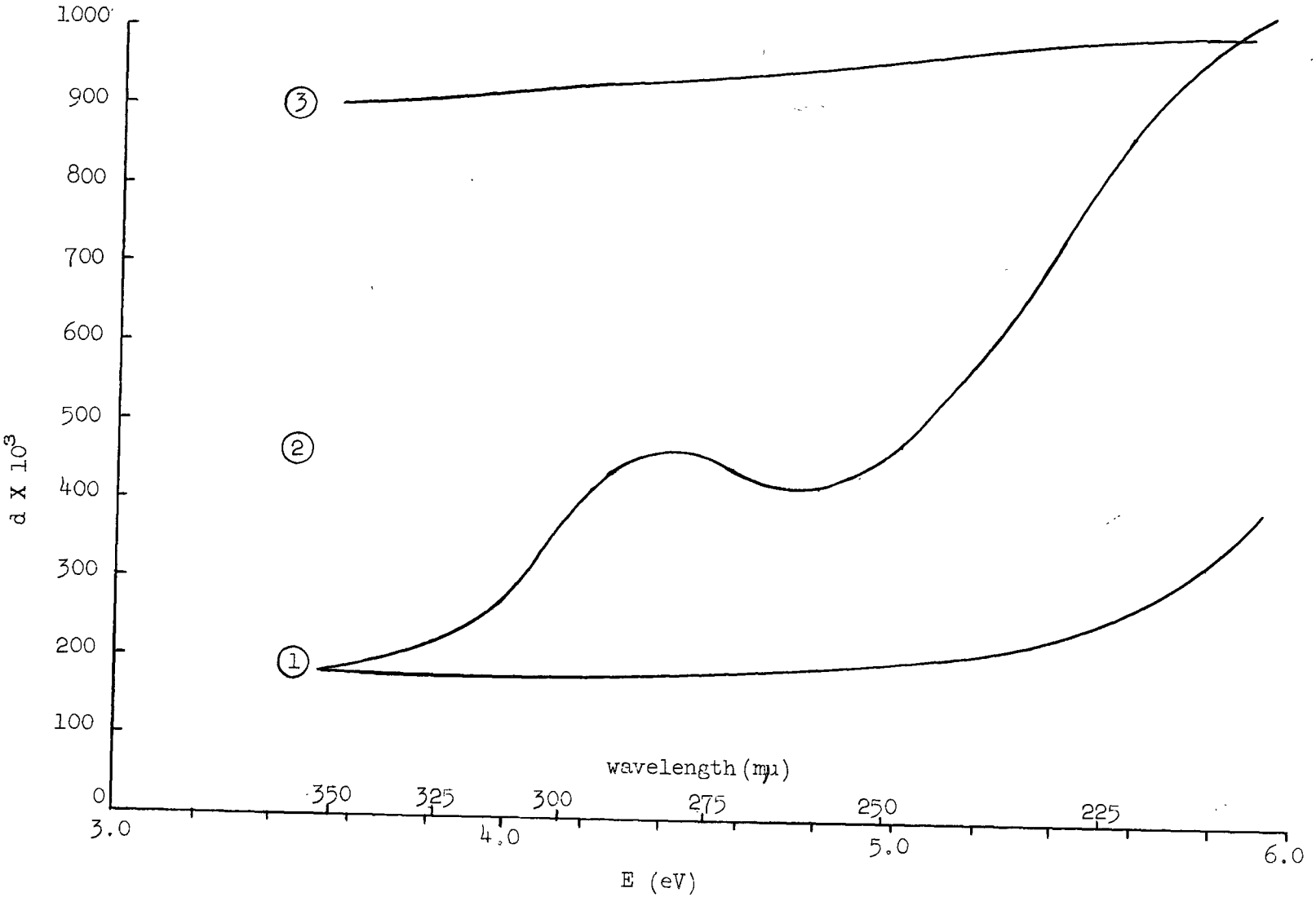

Figure 2. Absorption Spectra of MgO

2. It was assumed that no appreciable amount of absorbing species ~~were~~ was formed at wave-lengths ≥ 350 mμ and that any absorption in this region was due to small changes in transmitting and reflecting properties of the crystals caused by surface contamination. This correction was termed the "visible correction" and was calculated by the same procedure. Algebraic addition of this value to Δd_t served to match all spectra at 350 mμ.

2. Analysis of Individual Spectra:

Each peak followed a Gaussian relation[12]:

$$\Delta d\ (E) = \Delta do\ e^{[-k\ (E-Eo)^2]} \qquad \ldots\ldots\ (7)$$

where: E = energy

Eo = energy (or wave-length) at which the peak occurs,

Δdo = Δd at E = Eo

k = constant

The total spectrum was analyzed as follows[12]:

1) Assuming all absorption between 5.30 eV (234 mμ) and the peak at 5.75 eV (216 mμ) was due only to 5.75 eV centers, the graph of log $\Delta d(E)$ vs. $(\Delta E)^2$ was drawn (Figure 3.). All lines were essentially parallel except that for 150 minutes (dotted). For this time only the peak was found to occur at 5.70 eV (218 mμ). The data of Table II, Appendix D, replotted for the peak at 5.70 eV produced a straight line parallel to the others.

2) Assuming all absorption below 4.40 eV (282 mμ) was due only to the 5.75 and 4.40 eV centers (Table II, Appendix B.), similar curves were obtained for the 4.40 eV peaks. (Figure 4.)

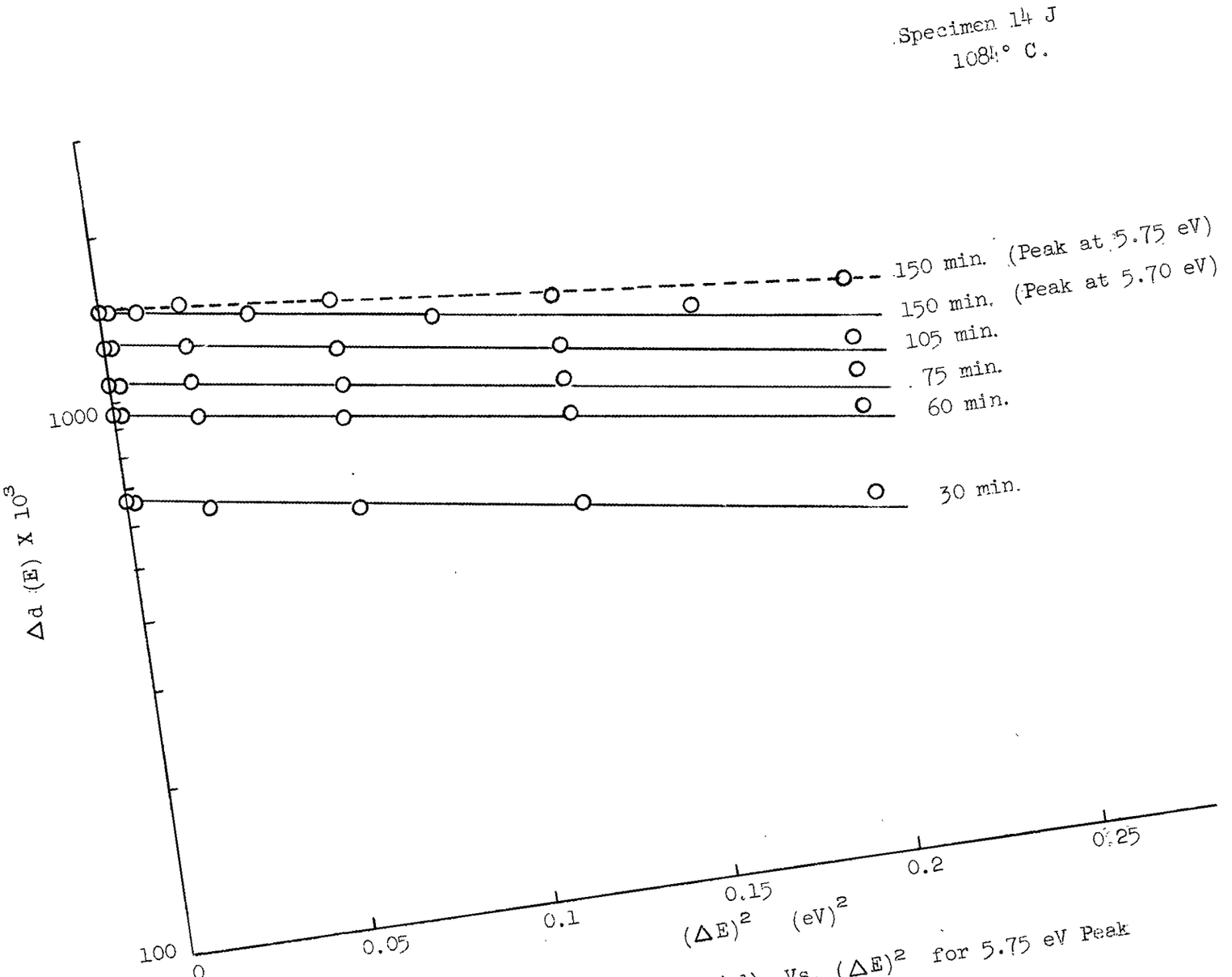

Figure 3. $\text{Log}_{10}(\Delta d)$ Vs. $(\Delta E)^2$ for 5.75 eV Peak

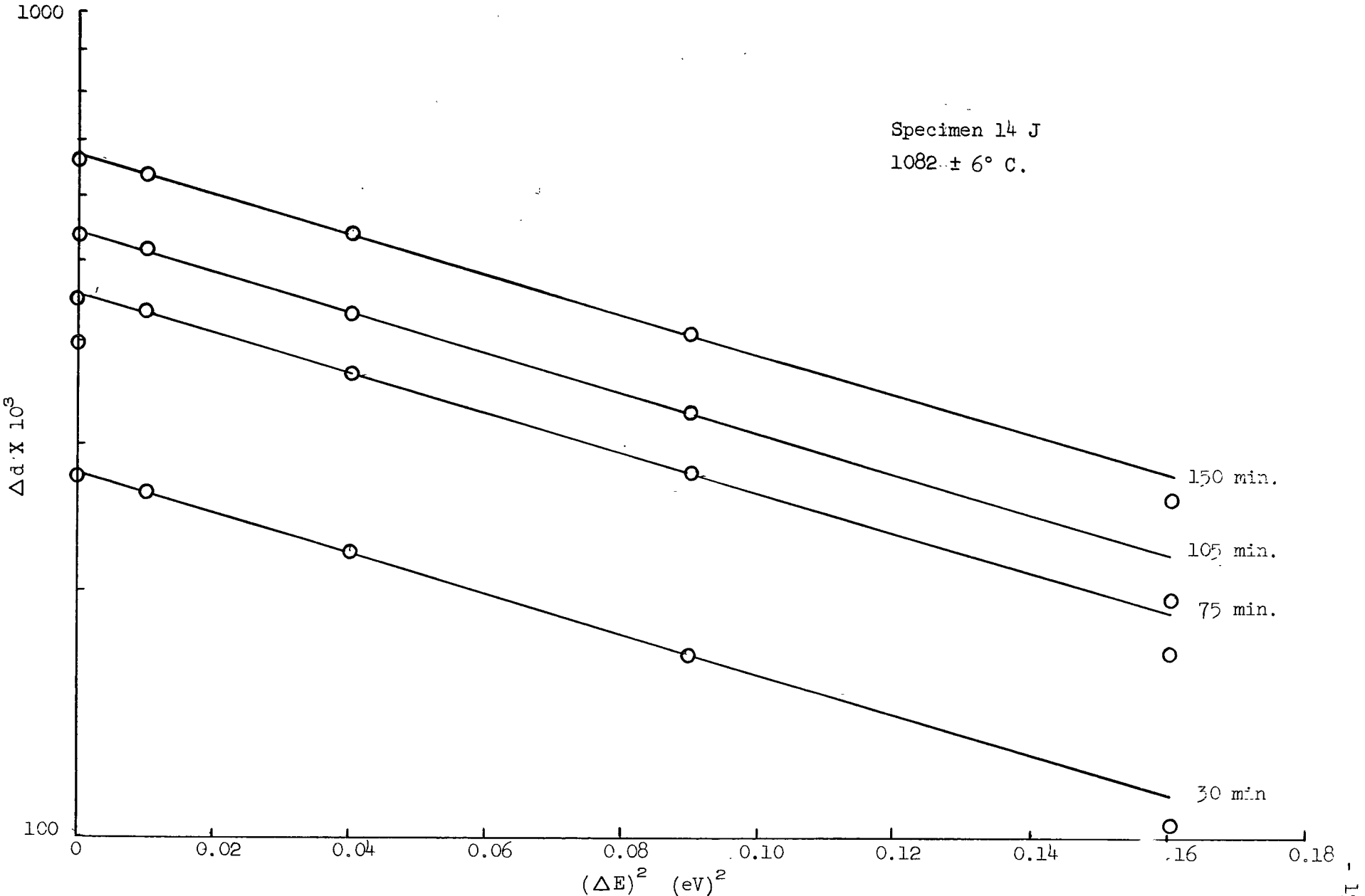

Figure 4. Log (Δd) Vs. $(\Delta E)^2$ for 4.40 eV Peak

3) A third peak was evident at 5.0 eV (248 mμ) when the Δd's calculated from the 4.40 and 5.75 eV peaks were subtracted from the observed density change (Table II). This peak was approximately Gaussian and the graphs for different times (Figure 5.) roughly parallel.

An analyzed spectrum is shown in Figure 6.

3. Diffusion Measurements

In a unidirectional diffusion mechanism which is governed by the conditions:

1) Initial:

$$C = 0 \text{ at } X > 0 \text{ and } t = 0$$

2) Boundary:

$$C = C_s \text{ at } X = 0 \text{ and } t > 0,$$

where: X = distance from the surface

s = surface

C = volume concentration of diffusing species

the total amount (M_t) of the diffusing substance (measured in terms of unit surface area) crossing the plane $X = 0$ in time t is given by[31]:

$$M_t = 2C_s \left(\frac{Dt}{\pi}\right)^{1/2} \qquad \ldots\ldots (8)$$

where: D = the diffusion coefficient

From equation (6), M_t is also given by:

$$M_t = (Cl_c)_t \quad \text{or,}$$

$$\Delta d_t = \frac{\epsilon M_t}{2.3} \qquad \ldots\ldots (9)$$

Equation (9) circumvents the necessity of knowing the time-varying quantity l_c.

TABLE II

Calculated Values of Δd_t for the 5.0 eV Peak

Specimen 14 J
60 minutes at 1082°C.

E	Δd_t obs'd X 10^3	Δd_t X 10^3 calc'd		Sum	Δd_t X 10^3
		4.40	5.75		5.0 eV
4.50	404	372	24	396	8
4.60	373	315	48	363	10
4.70	344	240	76	316	28
4.80	334	163	118	281	53
4.90	354	94	185	279	75
5.00	397	53	260	313	84
5.10	453	23	360	383	70
5.20	528	9	476	485	43
5.30	631	0	600	600	31
5.40	727	0	720	720	7
5.50	821	0	825	825	-4

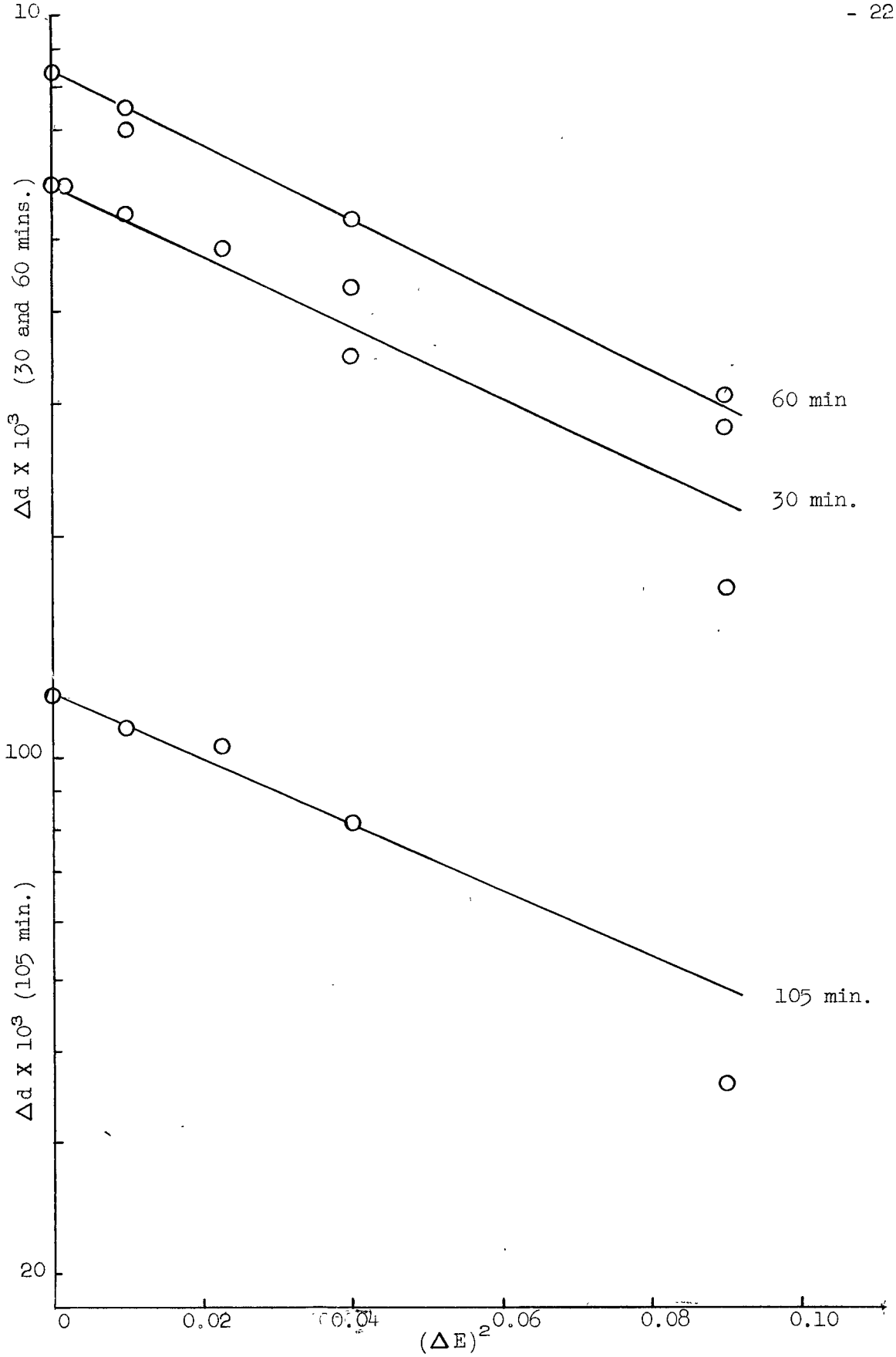

Figure 5. Log (Δd) Vs. $(\Delta E)^2$ for 5.0 eV Peak

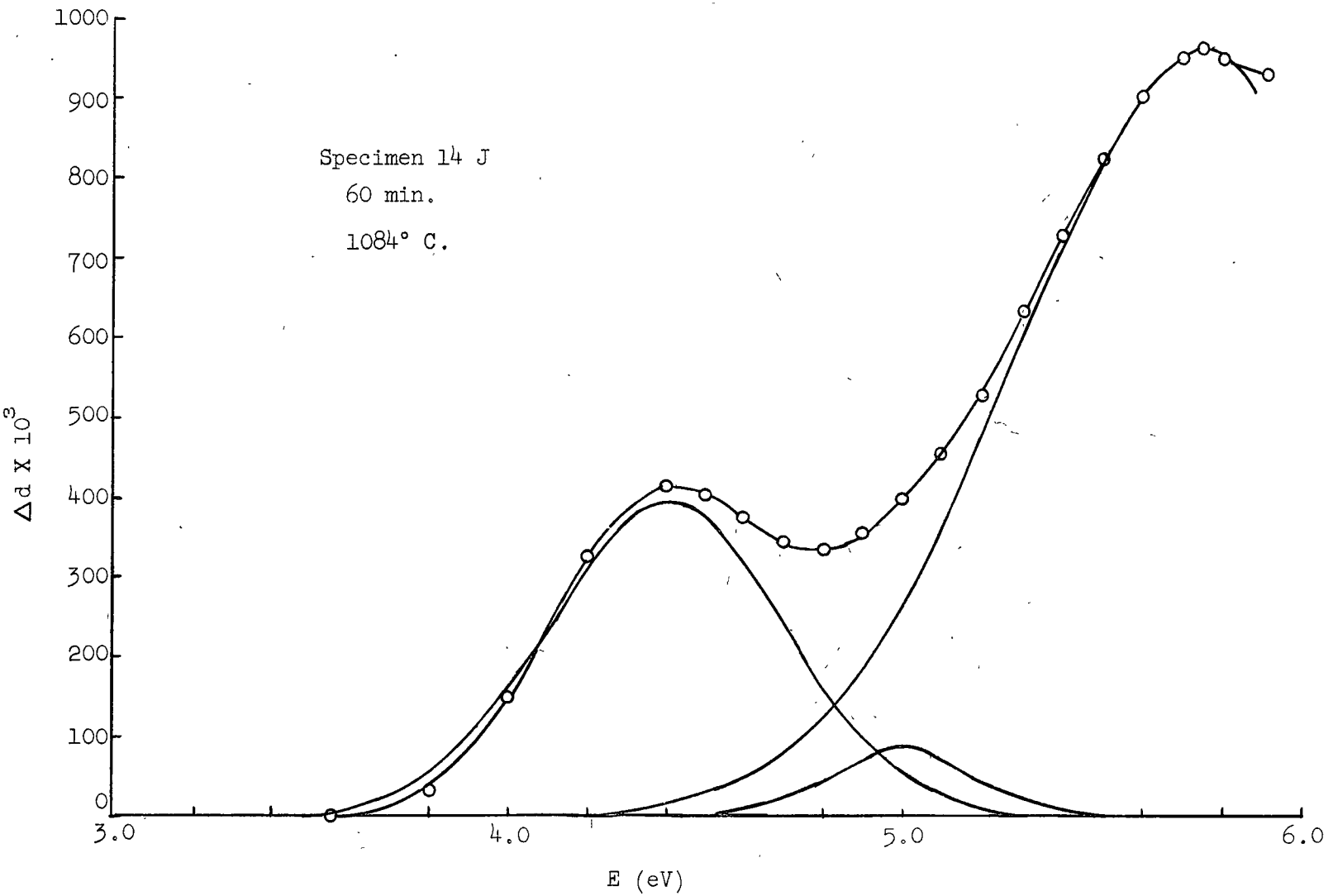

Figure 6. Analysed Spectrum Showing the Three Absorption Bands

From (8) and (9):

$$\Delta d_t = \frac{2 \epsilon C_s}{2.3} \left(\frac{D t}{\pi} \right)^{\frac{1}{2}} \quad \ldots\ldots (10)$$

Therefore, for a given temperature a plot of Δd_t vs. $t^{\frac{1}{2}}$ should yield a straight line with slope,

$$\frac{2 \epsilon C_s}{2.3} \left(\frac{D}{\pi} \right)^{\frac{1}{2}}$$

Such a plot yielded good straight lines for both the 4.40 and 5.75 eV peaks (Figure 7.). Although the points showed a great deal more scatter the 5.0 eV peak also followed this relationship (Figure 7.). Each 4.40 eV curve was uncorrected for the effect of the 5.75 eV peak. This correction shifted the Δd_t vs. $t^{\frac{1}{2}}$ curve downward; however, the slope within experimental error, was unaffected. The slope of each Δd_t vs. $t^{\frac{1}{2}}$ line was calculated using the method of least squares.

The straight line correlation indicated that the growth of the optical absorption peaks was governed by a diffusion mechanism. The activation energy of this process is defined by:

$$D = Do \; e^{\frac{-E}{RT}} \quad \ldots\ldots (11)$$

where: E = Activation energy

R = gas constant

T = temperature (°K)

Do = a factor which is generally thought to contain a frequency factor and to be a slowly varying function of temperature [32].

To determine E it was necessary to find the variation of C_s with temperature. The measurement of C_s at the lower temperatures was inconvenient owing to the length of time involved. A mechanism of formation and some aspects of the nature of the defects causing the absorption bands had therefore to be assumed so the measurements of C_s made at the higher temperatures could be extended to the lower temperatures.

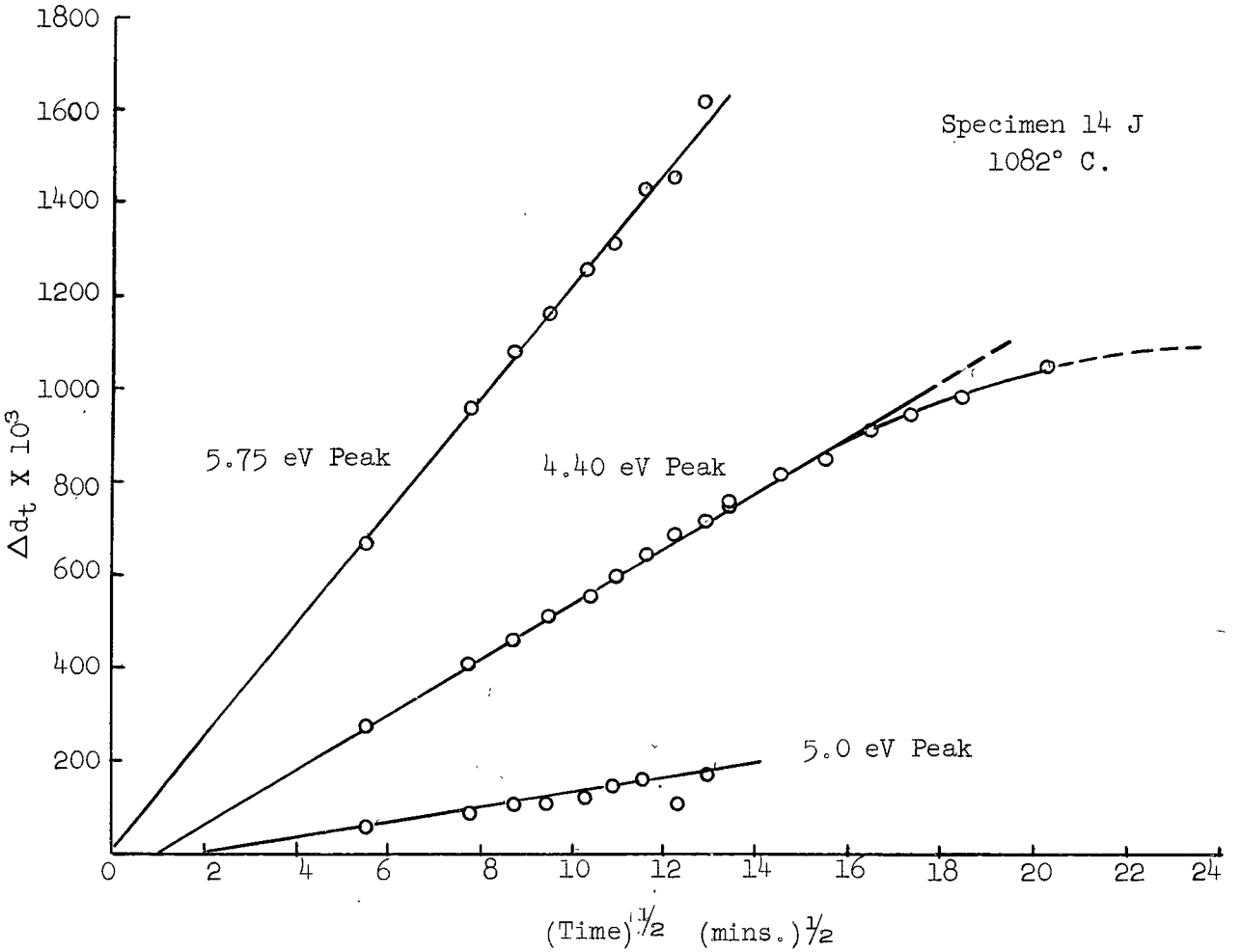

Figure 7. Typical Δd_t Vs. $t^{1/2}$ Curves

4. Mechanism of Formation of the Absorbing Species

Any mechanism to explain the formation of the absorbing species would be necessarily concerned either with the direct solution of oxygen in the magnesium oxide lattice or with the change in valence of iron from the +2 to the +3 state. Inevitably whichever reaction chosen would be the rate controlling step in the formation of the centers. Three such reactions appeared promising:

1. Direct solution (after Moulson and Roberts[28])
2. $2Fe^{+2} + \frac{1}{2} O_2 \rightleftharpoons 2Fe^{+3} + O^{=}$
3. $Fe^{+2} + \frac{1}{2} O_2 \rightleftharpoons Fe^{+3} + O^{-}$

Only reaction 3. appeared to fit existing experimental observations (See Discussion). Using this reaction as the terminal step of the overall mechanism:

$$\frac{1}{2} O_2 \text{ (gas)} \rightleftharpoons \frac{1}{2}[O_2] \text{ adsorbed}$$

$$\frac{1}{2} [O_2]_a \rightleftharpoons [O]_a$$

$$[O]_a + Fe^{+2} \rightleftharpoons Fe^{+3} + O^{-}$$

it may readily be shown by the addition of the individual free energy changes that if local equilibrium exists then:

$$-\Delta F^{\circ} = 4.575\ T \log_{10} K'$$

where: $$K' = \frac{[Fe^{+3}]\,[O^{-}]}{[Fe^{+2}]\,P_{O_2}{}^{1/2}} \qquad \ldots\ldots (12)$$

Further assumptions were made to allow calculations to be carried out using equation (12):

1) The concentration (C) of the absorbing species was defined by:

$$C = A\,[Fe^{+3}]\,[O^{-}] \qquad \ldots\ldots (13)$$

where: A = a proportionality constant.

2) The same defect center was responsible for the 4.4, 5.0 and 5.75 eV peaks.

3) The concentration of centers was small compared to the concentration of the Fe^{+2} ion. This implies that since:

$$[Fe^{+2}] + [Fe^{+3}] = [Fe]_{total}$$

then: $[Fe^{+2}] \simeq [Fe]_{total}$

Using assumptions (1) and (3) and replacing C by C_s in (13) then:

$$K' = \frac{C_s}{A\,[Fe]_t\, Po_2\, 1/2}$$

$$\text{since } C_s = \frac{2.3\,\Delta d_s}{\epsilon\, l_M} \qquad \ldots\ldots (14)$$

$$\text{then } K' A\epsilon = K = \left(\frac{2.3\Delta d_s}{l_M}\right)\left(\frac{1}{[Fe]_t\, Po_2\, 1/2}\right) \ldots\ldots (15)$$

Since all the quantities in (~~14~~ 15) were known, a $-\Delta F^\circ$ value could be calculated for each $\frac{\Delta d_s}{l_M}$ measurement. Haxby[22] found that both Fe and Mn caused the same ultraviolet peaks. The relative effect of Mn in terms of Fe was calculated using Haxby's results to be:

$$1 \text{ mole Mn} \equiv 0.063 \text{ moles Fe}$$

This fact was included in (~~14~~ 15) by replacing $[Fe]_t$ by $[Fe_t] + 0.063\,[Mn]$.

When $-\Delta F^\circ$ was plotted against T°K a straight line was obtained (Figures 8 and 9, Appendix E). Good agreement with Haxby's results for the 4.4 eV peak was also obtained; however, only those results from this investigation were used to determine the equation of this line.

Extrapolation of the line for each peak to lower temperatures thus produced values of $\frac{\Delta d_s}{l_M}$. Substituting (14) in to (10) and rearranging gave:

$$\frac{\Delta d_t}{t\ 1/2} = \left(\frac{\Delta d_s}{l_M}\right)\left(\frac{2}{\pi\ 1/2}\right) D\ 1/2 \qquad \ldots\ldots (16)$$

from which D could be readily calculated; a standard Arrhenius plot determined the activation energy for the diffusion process.

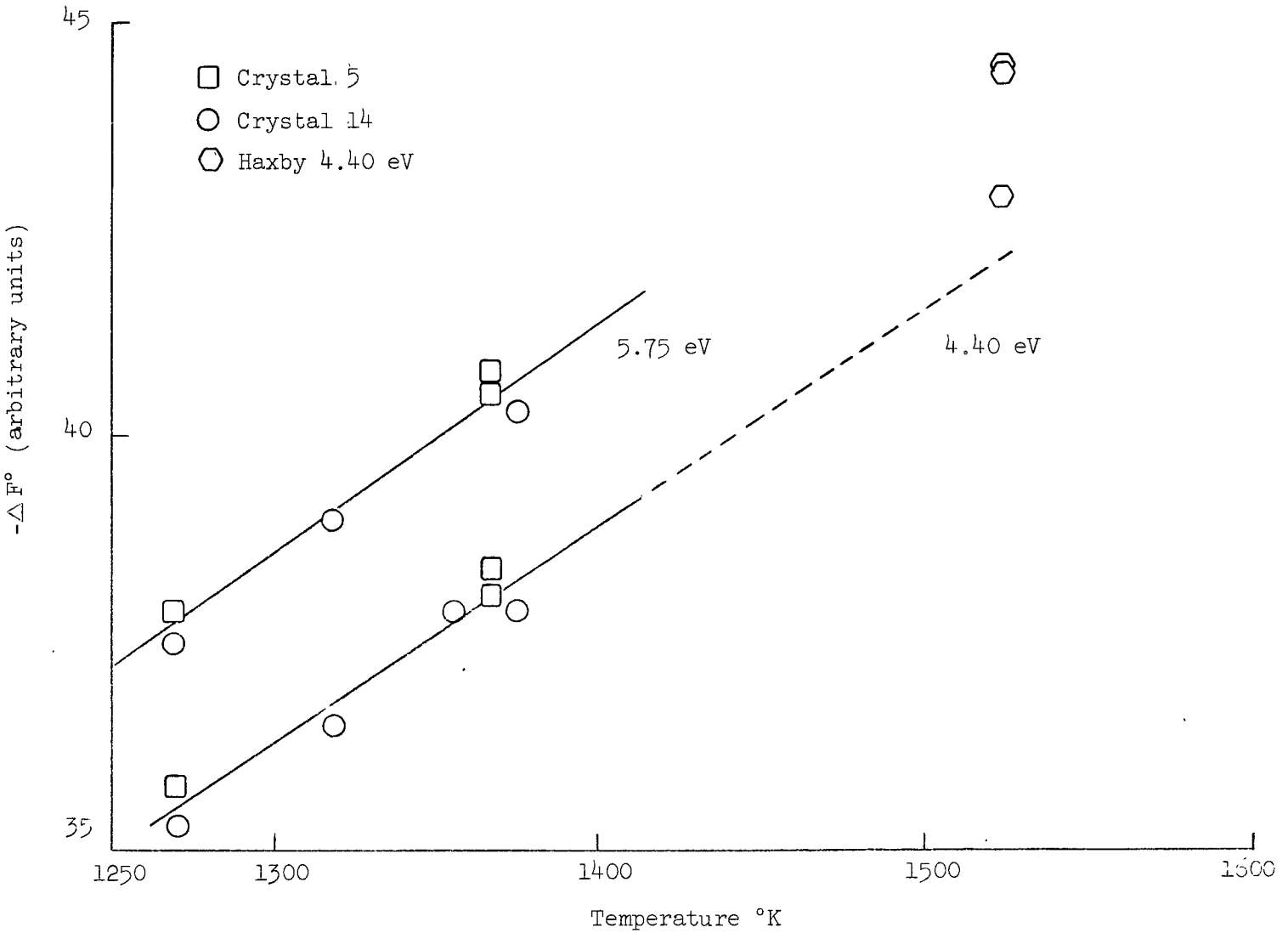

Figure 8. -△F° Vs. T°K for the 5.75 and 4.40 eV Peaks

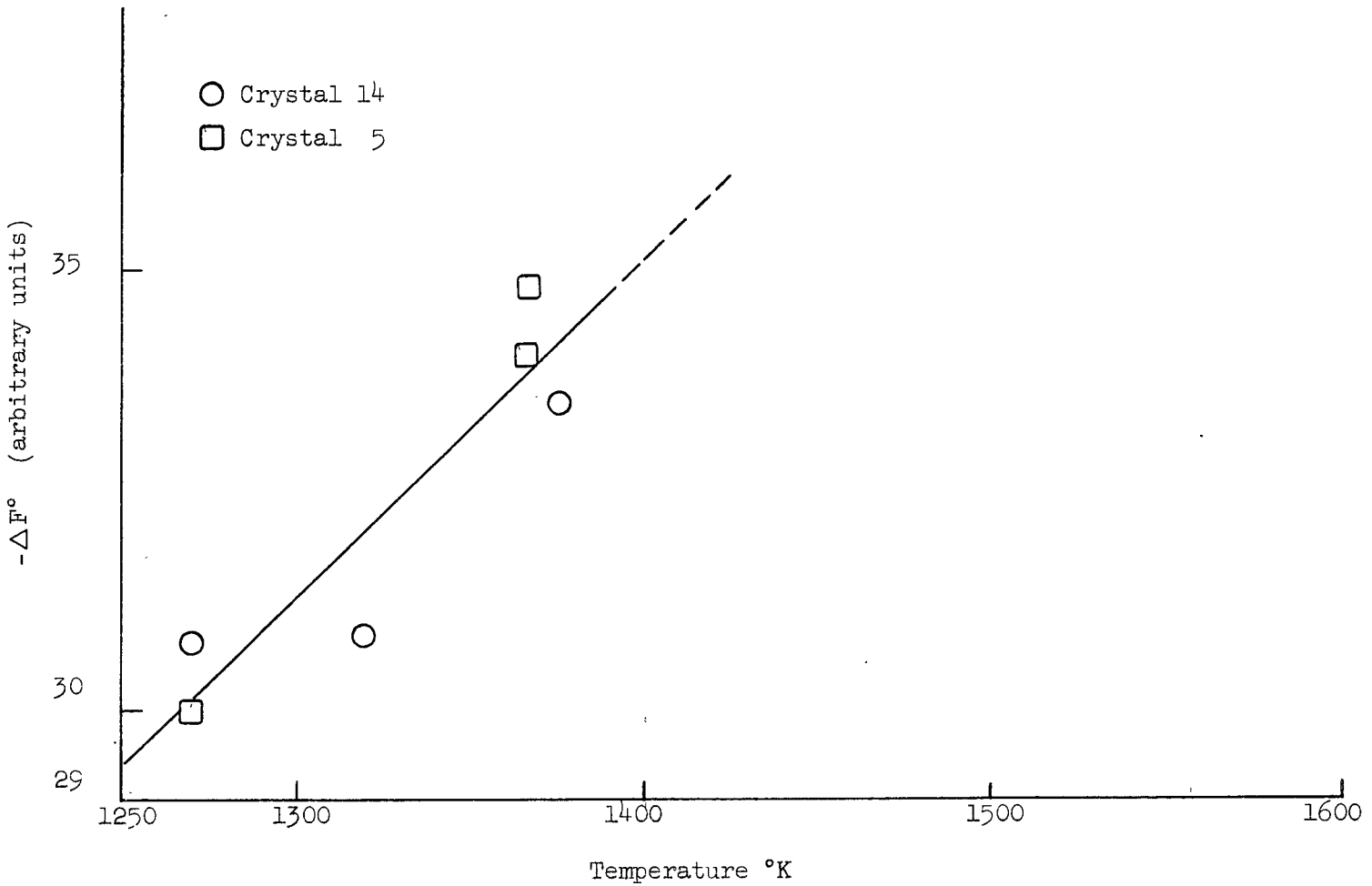

Figure 9. -ΔF° Vs. T°K for 5.0 eV Peak

B. Observations

1. Δd_t Vs. $t^{1/2}$ Curves

Breaks were observed in the lower temperature (~800 and ~850° C.) curves. These breaks exhibited an erratic nature; for example, they occurred at approximately 120 hours at 842° C. under one atmosphere oxygen and approximately 196 hours at 795° C. in air for both the 4.40 and 5.75 eV peaks. However, no breaks occurred at 850° C. in air (up to 139 hours) whereas at 792°C. in oxygen produced one at 25 hours for the 4.40 eV peak only. Furthermore, the readings at longer times showed an increasing rate of growth of the peaks. These readings generally followed a linear relation of Δd_t vs. $t^{1/2}$; however, the measurements beyond 196 hours at 795° C. in air evidently did not. (See Figures 10 and 11).

One specimen exhibited similar behaviour at a higher temperature (5 C. 1,996° C., air; Figure 12.). This break occurred at 100 hours (in the near-saturation region); however, succeeding points followed a linear relationship with a drastically decreased slope until readings were stopped at 383 hours.

Both the erratic behaviour of the discontinuities and the fact that the total times of some low temperature runs were not comparable (e.g. 850° C. Figure 10.) made an interpretation very difficult. Possible reasons for these changes could be:

1) the errors inherent in measuring the small changes (at 800° C.)
2) the effect of surface contamination
3) a change in diffusion mechanism
4) the effect of further optical (defect) structure in the visible range or in the region below 212 mμ.

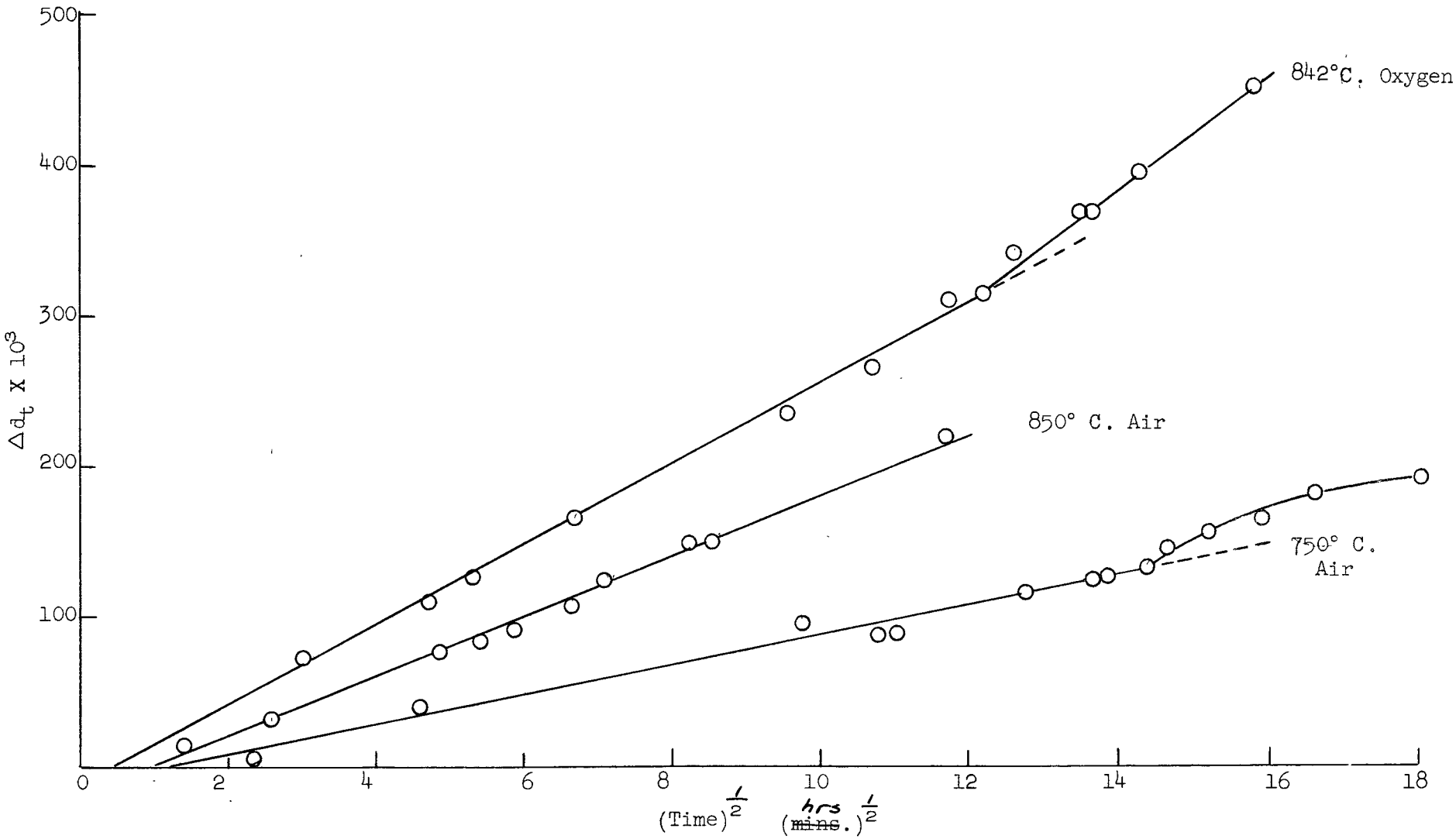

Figure 10. Plots of Δd_t Vs. $t^{1/2}$ Showing Two of the Discontinuities Observed for the 4.40 eV Peaks.

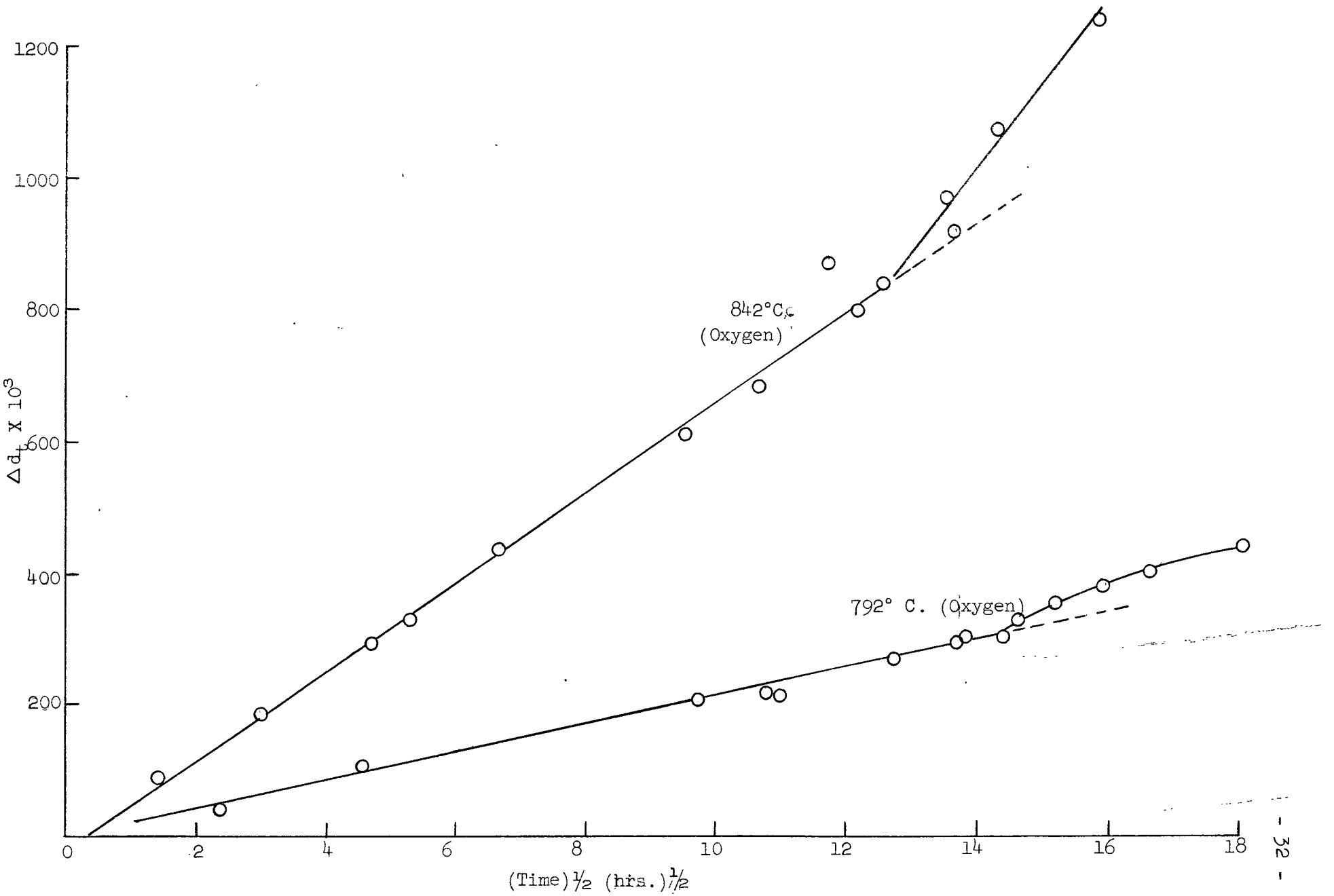

Figure 11. Two Discontinuities Observed in the Plots of Δd_t Vs. $t^{1/2}$ (5.75 eV Peak)

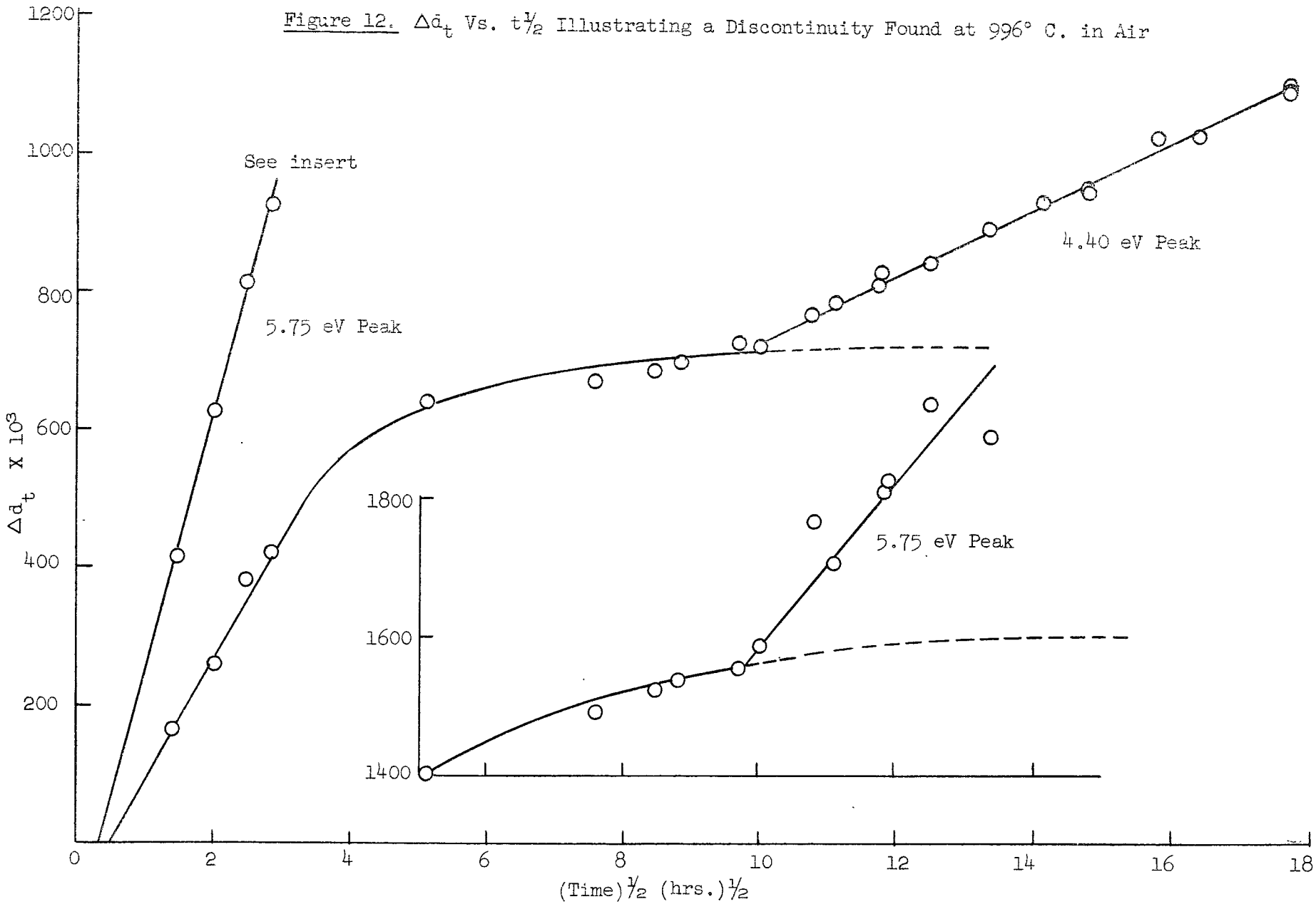
Figure 12. Δd_t Vs. $t^{1/2}$ Illustrating a Discontinuity Found at 996° C. in Air
1200
1000
800
600
400
200
Δd_t X 10^3
See insert
5.75 eV Peak
4.40 eV Peak
1800
1600
1400
5.75 eV Peak
0
2
4
6
8
10
12
14
16
18
(Time)$^{1/2}$ (hrs.)$^{1/2}$

2. Microscopic Examination

Cursory microscopic examination was performed. The following observations were made:

1) There appeared to be no appreciable or consistent differences between the vacuum annealed and the oxygen-treated specimens when examined under ordinary light up to X 200 magnification.

2) Under polarized light the oxygen-treated crystals exhibited stress patterns like those shown in Figure 13c. No stresses were evident in either the vacuum annealed specimens (13b.) or the as-cleaved material (13a.)

3. Yellow Crystals

A number of platelets cleaved from crystal 19 were vacuum annealed under the same conditions as those used for crystals 5 and 14. A visible and infra-red as-received spectrum of one such platelet showed optical structure only near 395 mμ (3.2 eV). This structure was removed by vacuum annealing; however, a much longer anneal (>5 hours) than usual was necessary to eliminate the ultraviolet structure in platelets of approximately the same thickness as those cleaved from crystals 5 and 14.

The as-received spectrum of a thick (0.304 X 0.356 inch) yellow crystal was also recorded. This spectrum showed definite shoulders at 475 (2.7 eV) and 395 (3.2 eV) mμ. Other specimens from the "impure" crystal exhibited definite peaks near 2690 and 475 mμ and a shoulder near 400 mμ. These peaks and shoulders were probably caused by impurities[20,21,22] since colorless specimens of comparable thickness showed no such structure.

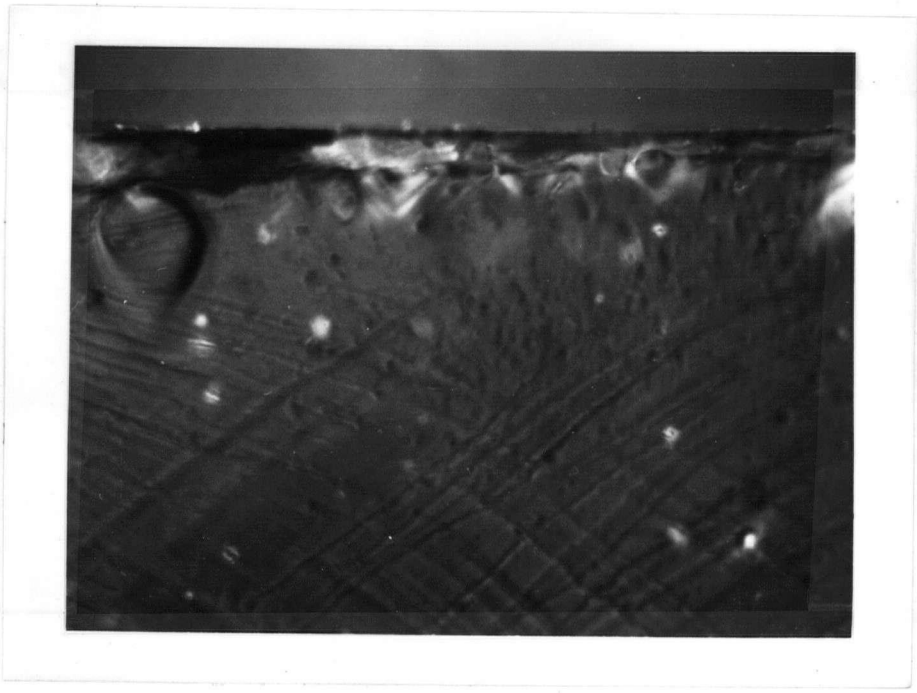

Figure 13a. Typical As-cleaved Specimen under Polarized Light

(X100)

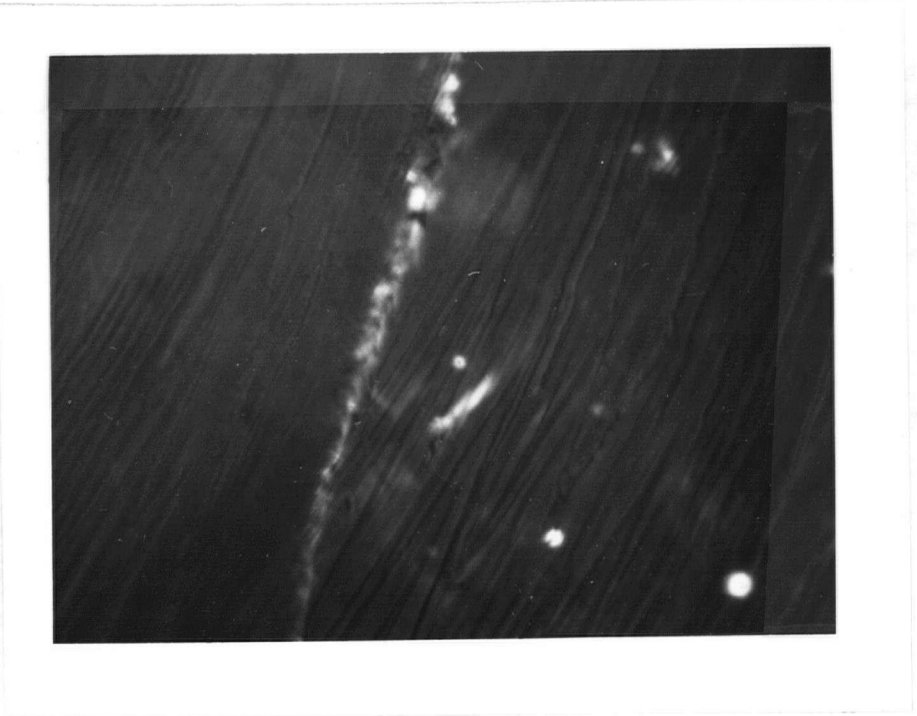

Figure 13b. Typical Vacuum Annealed Specimen under Polarized Light

(X 100)

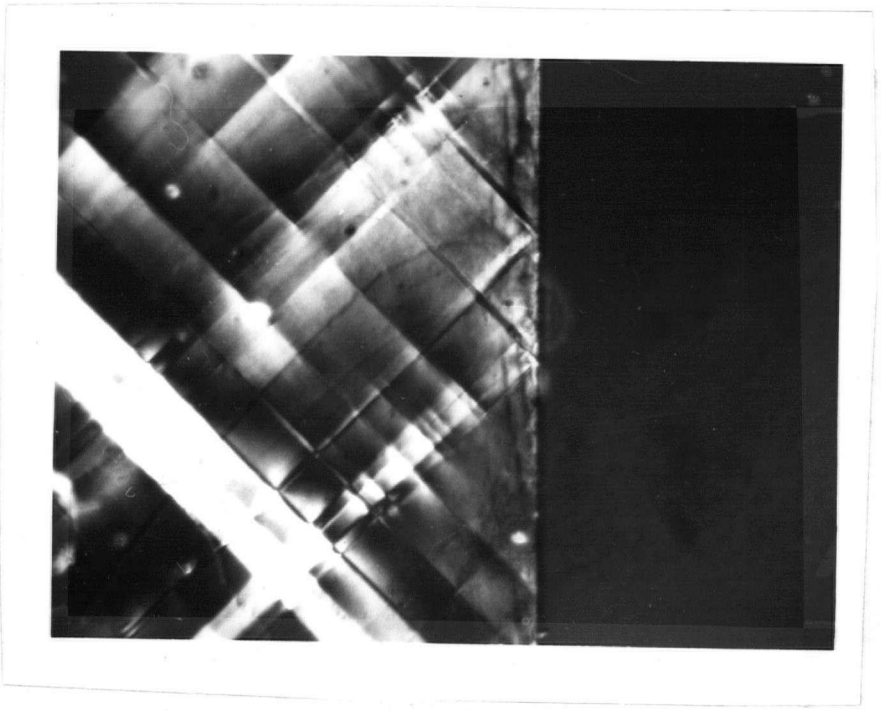

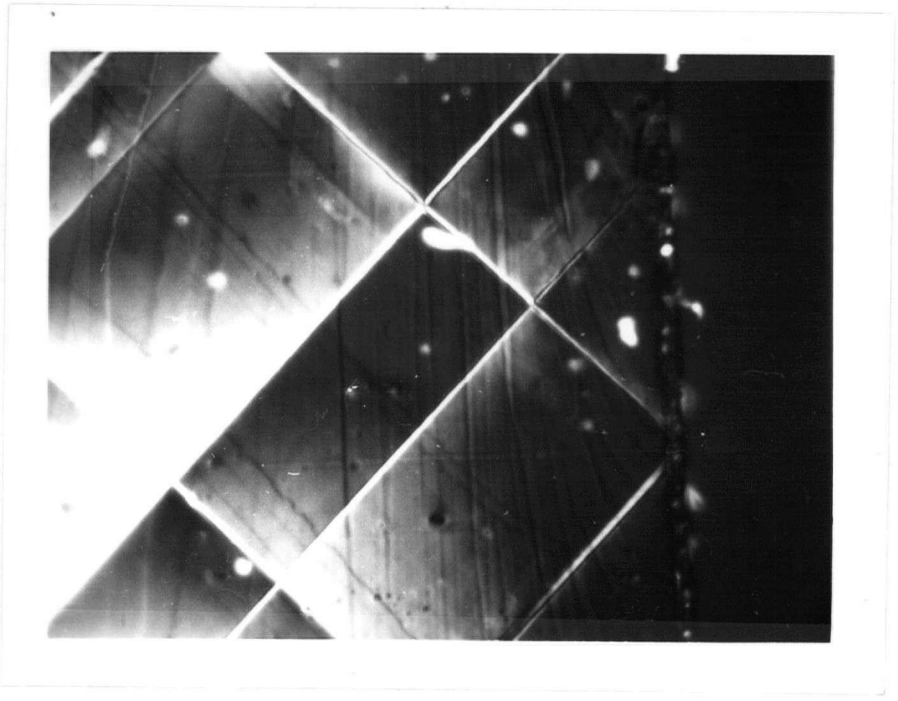

Figure 13c. Two Stress Patterns found in a Heat-Treated Specimen
5 D 1 - 22 hours at 1094° C. in Air
(X 100)

C. Summary of Results

1. Reproducibility

A number of factors affected not only the reproducibility but also the amount of error inherent in the diffusion measurements:

1) By reversing the specimen in the light beam of the spectrophotometer an optical density difference of 0.05 could be obtained.

2) If the specimen face was not perpendicular to the light path or at least the same position not reproduced then small variations in optical density would result.

3) Any grease on the specimen faces could also produce variations in ultraviolet optical density.

4) Changing furnace position could result in about ± 20° C. difference in temperature in the horizontal direction. The vertical direction was not as critical and was within the recorded temperature fluctuations.

By rendering all these factors essentially constant by a standardized experimental procedure yielded good reproducibility. Table III shows two examples of the reproducibility of the slope of the Δd_t vs $t^{1/2}$ curves.

TABLE III

Reproducibility of Slopes of Δd_t Vs. $t^{1/2}$ Curves

Specimen	Atmosphere	Thickness in inchs	Temperature (°K)	Slope X 10^3 4.4 eV peak
5 C 2	air	0.0129	1367	48.3 $min^{-1/2}$
5 D 2	air	0.0181	1367	47.4 $min^{-1/2}$
5 J	air	-	1182	46.9 $hr.^{-1/2}$
5 H 1	air	-	1182	47.3 $hr.^{-1/2}$

The cooling rate effect, although determined indirectly appeared to be negligible. Moreover, changes in the flow rate of the oxygen through the furnace also had no noticable effect (Figure 14.).

2. Diffusion Measurements

a) The 4.40 and 5.75 eV Peaks

A typical family of Δd_t vs. $t^{1/2}$ curves for different temperatures is shown in Figure 15. The slopes of these lines together with the $\frac{\Delta d_s}{I_M}$ values calculated using the proposed mechanism produced the logarithm of the diffusion coefficient (D) vs. $\frac{1}{T}$ plot shown in Figure 16. The two important features of this plot were:

1) The activation energy was found to be (see also Appendix F)

$$77.0 \pm 1.4 \text{ kcals}$$

which is in close agreement with the value determined by Lindner and Parfitt[33] for the diffusion of Mg^{28} in magnesium oxide. Their value was:

$$79.0 \pm 3.0 \text{ kcals}$$

The value determined by this investigation is also in agreement with that estimated by Weber[5] and Shepherd[22] of

$$\sim 3.4 \text{ eV} = 78.5 \text{ kcals}$$

The Do value was calculated to be 1.7×10^5 in contrast to the value of 0.249 quoted by Lindner and Parfitt.

2) The values of D calculated from measurements on the 4.40 and 5.75 eV peaks were both represented by the same straight line. This was also the case for both sets of specimens; each set being heated under a different pressure and each set having different amounts of iron and manganese.

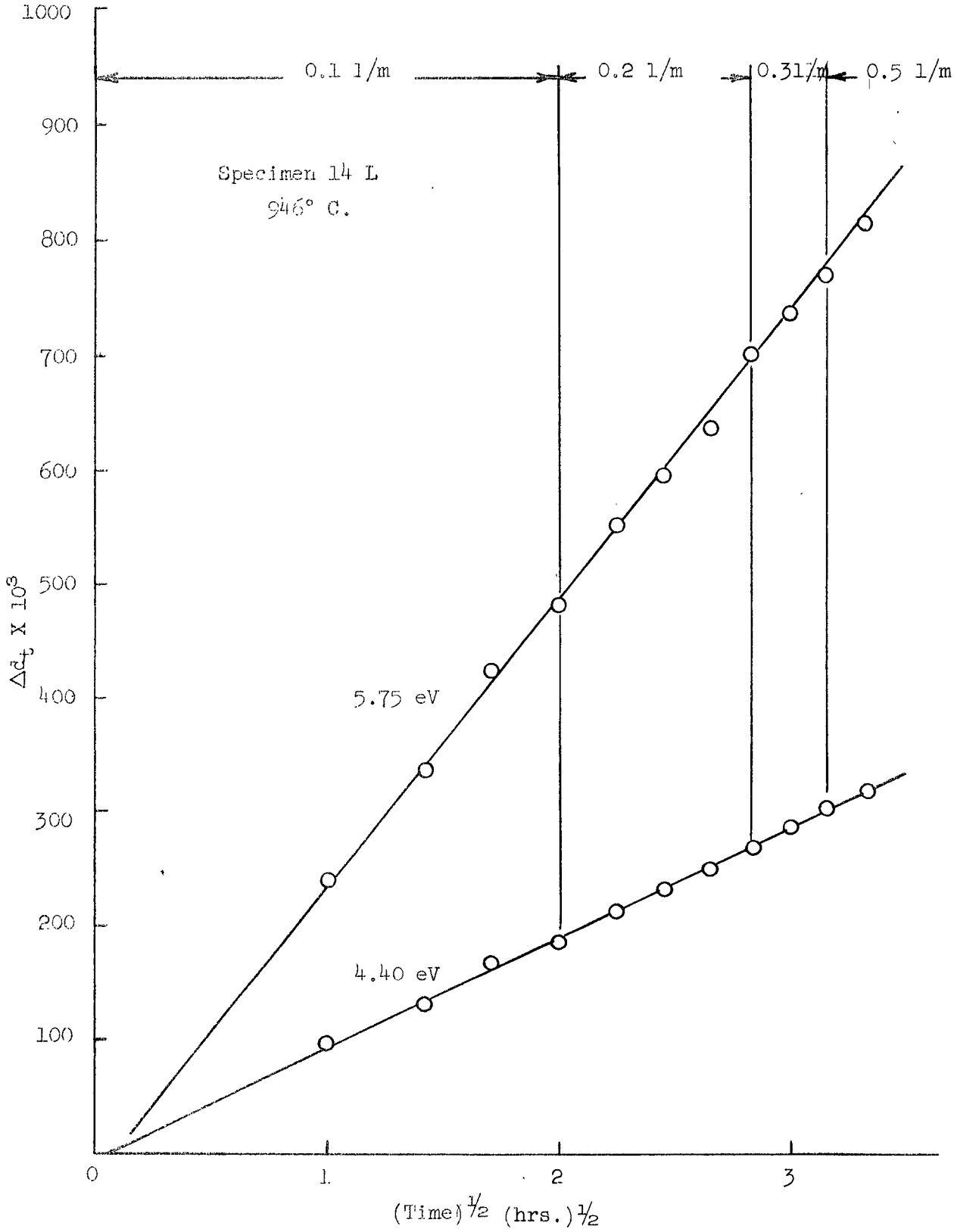

Figure 14. Effect of Flow Rate

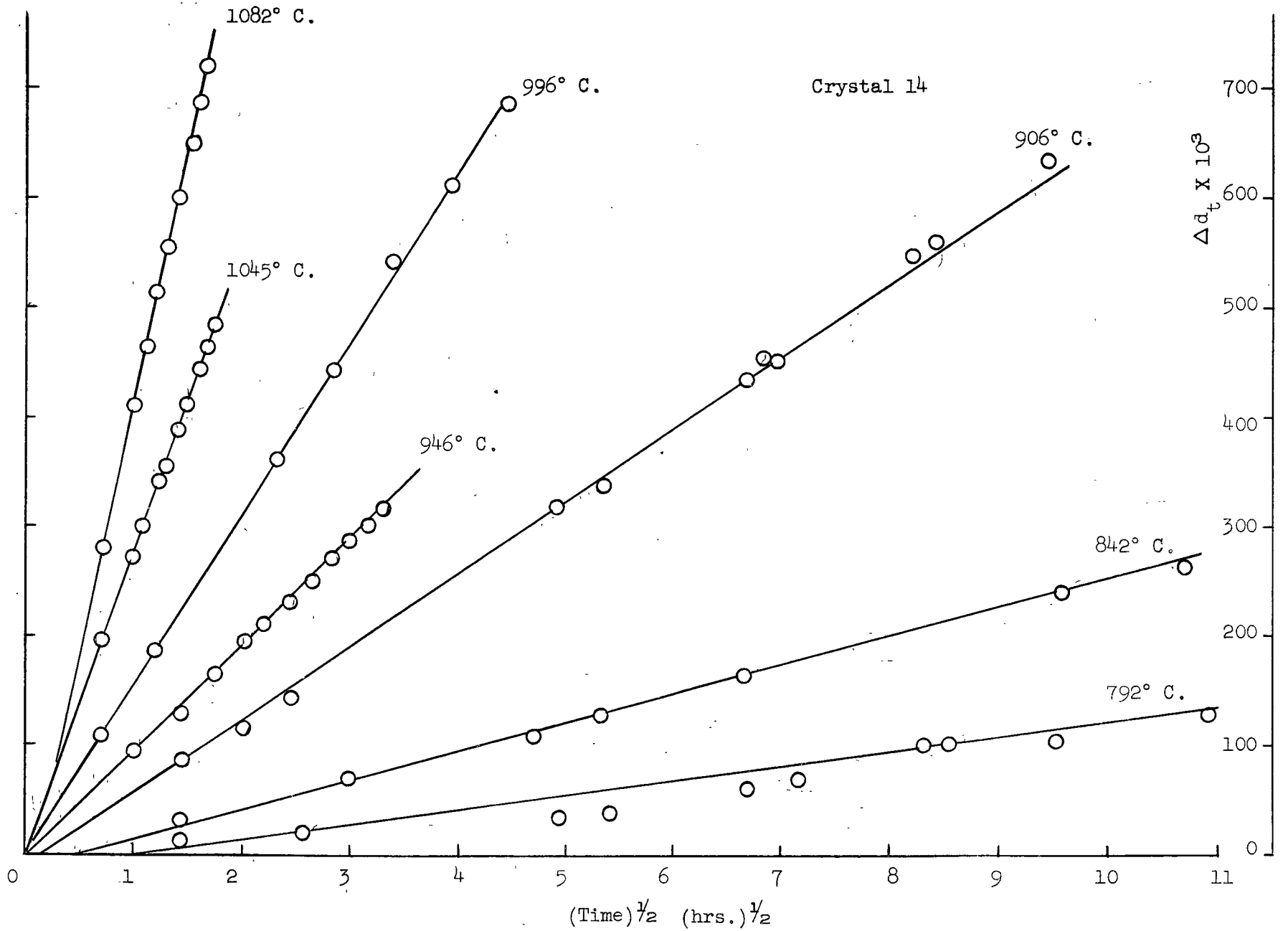

Figure 15. Plots of Δd_t Vs. $t^{1/2}$ for Different Temperatures.

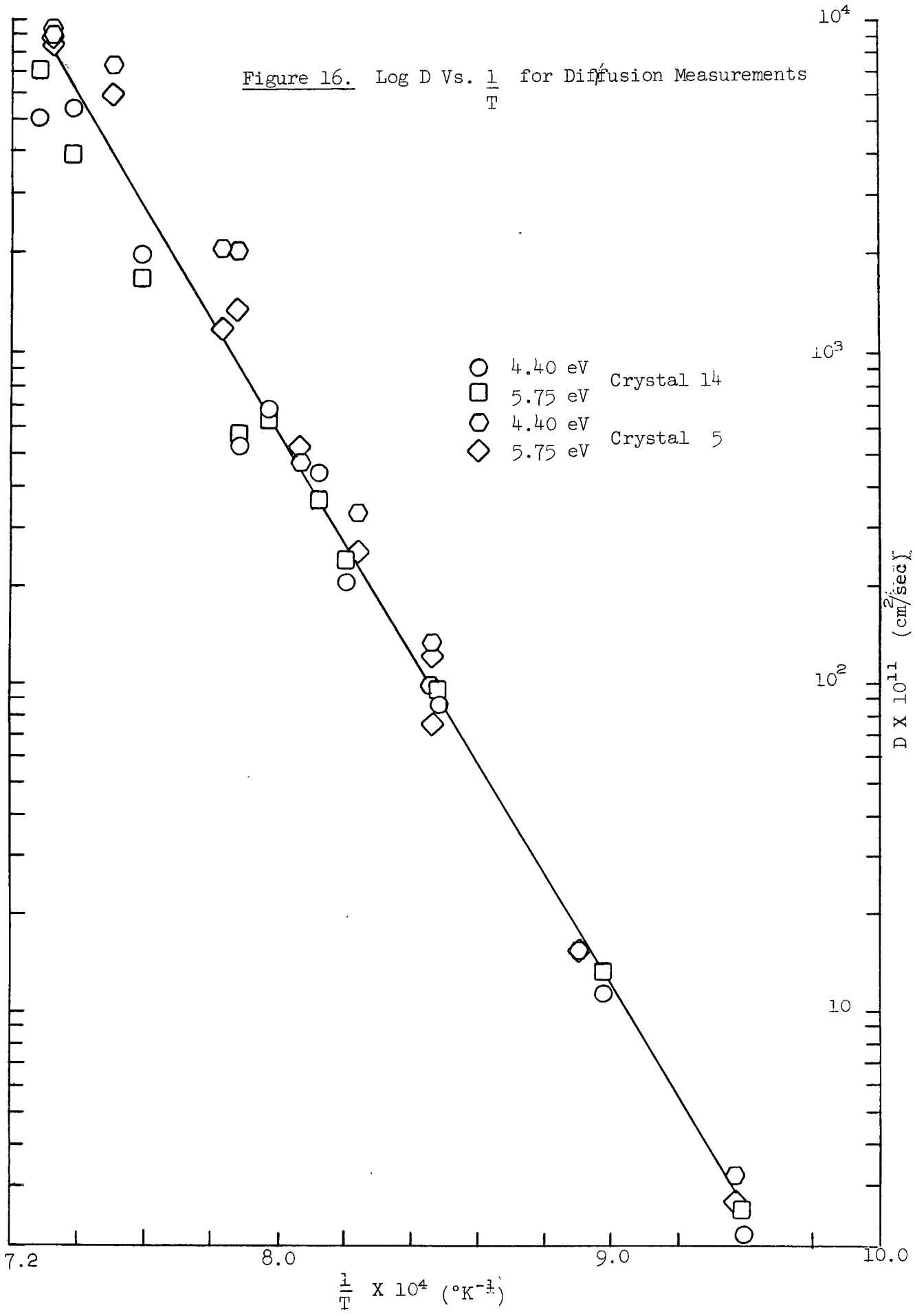

Figure 16. Log D Vs. $\frac{1}{T}$ for Diffusion Measurements

b) The 5.0 eV Peak

Similar calculations using measurements on the 5.0 eV peak were not as successful. Table IV shows D determined from 5.0 eV peak data compared to the D's obtained from the 4.4 and 5.75 eV peak data. The inconsistency of the 5.0 eV peak results was probably caused by the errors inherent in determining small changes between two large numbers. This situation was most apparent at the lower temperatures (<1232 °K). The 5.0 eV results were omitted when the activation energy was calculated.

It was also found that values of $\frac{\Delta d_s}{l_M}$ calculated using Figure 9. decreased rather than increased with decreasing temperature (see Table IV, Appendix E.)

TABLE IV

Comparison of D-Values Calculated from the Three Peaks

Specimen	Temperature °K	D X 10^{11} (cm^2/sec) 4.40 eV	5.75 eV	5.0 eV
14 J	1355	545.0	392.0	913.0
14 M	1318	198.0	167.0	242.0
14 Q	1269	52.6	58.2	65.9
14 N	1255	69.2	65.1	77.3
14 D	1232	44.2	36.5	178.0
5 D 2	1367	902.0	876.0	1747.0
5 C 2	1367	936.0	832.0	590.0

IV. DISCUSSION

A. General

The observations and the results of this investigation as well as those cited from other works appear to infer that most if not all, of the optical absorption structure in magnesium oxide between 212 and 2800 mμ is caused by impurities. In particular, the two ultraviolet bands at 4.40 and 5.75 eV about which this project was primarily concerned may be attributable to an oxidation reaction involving a transition of Mn and Fe from the +2 to the +3 state[8,12,22]. Moreover, the results indicate that a diffusion process accompanies the reaction. This diffusion process has been observed by others[5,22].

Both the 5.75 and the 4.40 eV peaks apparently have the same activation energy for diffusion (Figure 16.); it may then be concluded that the same defect and the same diffusion process causes both these bands. In addition, since the calculation of the activation energy was based on the assumption that the above oxidation reaction was involved indicates that these two peaks are in fact, both due to Fe^{+3} (and Mn^{+3}).

Although the 5.0 eV peak is evident under the same conditions as the other two, the inconsistency of and the error in calculations for this peak do not lend themselves to the drawing of similar conclusions. Certainly this band could well be due to the same impurity reaction; however, the existence of a Cr^{+2} peak at 5.0 eV[17] and the possibility of another reaction of the type[22]:

$$Cr^{+3} + Fe^{+2} \longrightarrow Cr^{+2} + Fe^{+3}$$

occurring during the oxygen treatment would make it difficult to draw such a definite conclusion.

B. Mechanism of Formation of the Absorbing Species

The diffusion results indicate that the postulated mechanism of formation of the absorbing species although over-simplified, had some basis

in fact; all the measurements of the diffusion coefficient (D) made under different conditions could be represented by one straight line. Apart from this, the mechanism also incorporates some desirable qualities.

The importance of the adsorption of oxygen in the formation of the centers[5,22] is included. The adsorption process is implied from the dependence of the saturation density of centers on the logarithm of the oxygen pressure (the Temken isotherm[34]). Moreover, the observation that the saturation level decreases as the temperature increases is predicted by the mechanisms for the 4.40 and 5.75 eV peaks but evidently not for the 5.0 eV peak (See Figures 8 and 9; Appendix E).

Results of studies of the exchange reaction of O^{18} on the surface of sintered magnesium oxide[35] indicated that the amount of coverage by adsorption was small (ca. 0.1%). Also, the adsorption process consisted of the dissociation of the oxygen molecule and the migration of a portion of the ad-atoms over the surface to suitable exchange sites; the exchange involved a transfer of electrons between the ad-atoms and either a surface oxygen ion or an appropriate defect. Both these results imply that the probability of the formation of an absorbing center through the reaction of Fe^{+2} and the adsorbed oxygen is small and hence provides a partial justification for the approximation:

$$[Fe^{+2}] \simeq [Fe]_{total}$$

The reaction assumed to form the centers involved the formation of the O^- ion. Intuitively, oxygen in this state would be unstable. However, the total reaction could be

$$2Fe^{+2} + \tfrac{1}{2}O_2 \rightleftharpoons 2Fe^{+3} + O^{=}$$

This could occur in two stages[36]:

1) $Fe^{+2} + \frac{1}{2}O_2 \underset{k_2}{\overset{k_1}{\rightleftharpoons}} Fe^{+3} + O^-$ (slow)

2) $Fe^{+2} + O^- \xrightarrow{k_3} Fe^{+3} + O^=$ (fast)

with 1) being the rate-controlling step. The first-order nature of the reaction with respect to the iron content can then be illustrated as follows:

1) $\frac{dO^-}{dt} = - k_2 [Fe^{+3}] [O^-] + k_1 [Fe^{+2}] Po_2 \frac{1}{2}$

2) $\frac{dO^=}{dt} = - k_3 [Fe^{+2}] [O^-]$

where k_1, k_2 and k_3 are rate constants. Assuming the steady-state approximation:

$$\frac{d[O^-]}{dt} \simeq 0$$

then

$$[O^-] = \frac{k_1 [Fe^{+2}] [Po_2 \frac{1}{2}]}{k_2 [Fe^{+3}] + k_3 [Fe^{+2}]}$$

Substituting this expression into the overall rate equation for the formation of the stable $O^=$ ion:

$$\text{rate} = k_3 [Fe^{+2}] [O^-]$$

gives:

$$\text{rate} = \frac{k_3 k_1 [Fe^{+2}]^2 Po_2 \frac{1}{2}}{k_2 [Fe^{+3}] + k_3 [Fe^{+2}]}$$

if $k_2 [Fe^{+3}] << k_3 [Fe^{+2}]$

then $\text{rate} \simeq k_1 [Fe^{+2}] Po_2 \frac{1}{2}$

The observation that the activation energy for the diffusion process is the same as that for Mg in magnesium oxide suggests that the oxidation of two Fe^{+2} ions may be accompanied by the migration of one magnesium ion to the surface thus leaving behind a positive ion vacancy. From the work of Wertz et al[18] on X-irradiated crystals, the vacancy should be located adjacent to a tri-valent impurity ion-assumed in this case to be Fe^{+3}. Further credence

is thus given the proposed mechanism when it is realized that the concentration of Mg^{+2}(excess) vacancies should be equivalent to the number of O^- ions formed. Therefore the defect center may be defined as

$$(Fe^{+3} \cdot V\ Mg^{+2})$$

rather than $(Fe^{+3} \cdot O^-)$

The proportionality constant, A, is then unnecessary since the Fe^{+3} concentration measured is now only that concerned with the defect center itself. It is interesting to speculate that the generation of new lattice sites by the diffusion of Mg to the surface would result in an expansion of the crystal (The expansion of thin crystals of NaCl and KCl due to the formation of F-centers by X-irradiation has been measured[37].) The expansion could then conceivably produce the stress patterns shown in Figure 13. However, the patterns may be due to another mechanism such as thermal cycling.

The proposed mechanism accounts for some experimental observations but is found lacking in other respects. For instance, the possibility of the simultaneous depletion of the Fe^{+3} due to reaction with Cr^{+2} [22] is ignored. Similarly no account is taken of the possible agglomeration of centers or the migration of positive ion vacancies present in the crystal before heat treatment, to Fe^{+3} sites to form centers. Moreover, it does not explain the discontinuities observed in the Δd_t vs. $t^{1/2}$ curves.

The possibility of the diffusion of oxygen into the crystals with subsequent adsorption on the inner surfaces[5] and reaction with Fe^{+2} is also not evident in the mechanism. This feature is a possible alternative to the migration of magnesium to the surface since the same equations used to explain the diffusion process could also be applied to diffusion of oxygen with simultaneous reaction and immobilization[31]. This would imply an instantaneous reaction and the modification of D to $\frac{D}{R+1}$ where R is defined by: $S = RC$

where: S = the concentration of immobilized substance

This would affect the activation energy only if R varied with temperature; the Do value, however, would be different from that calculated using the proposed mechanism.

Perhaps the greatest weaknesses arise from the small variation in conditions under which the measurements of D were taken and the assumption inherent in the extrapolation of the lines in Figure 8 to lower temperatures that the same proposed reaction occurs below ca. 1000° C. Furthermore the formulation of the mechanism is based on three groups of readings over a range of only 100° C.; however, the agreement obtained with Haxby's results at a higher temperature (1523° K.), a lower pressure (15 mm Hg) and a wider composition variation does add some credibility to the interpretation.

V. CONCLUSIONS

1. A technique has been developed (used previously by Moulson and Roberts[28]) to study a diffusion process occurring in magnesium oxide single crystals. This was done utilizing optical absorption measurements only. The usefulness of the technique was found to be dependent on the ability to measure the optical density of the saturated state.

2. A mechanism of formation of the absorbing species was postulated. With this mechanism the saturation states at lower temperatures could be calculated. The times needed to reach saturation at these temperatures was found to be prohibitive.

3. The activation energy of the diffusion process was found to be 77 ± 1.4 kcals per mole. This value was the same as that found for Mg^{28} in MgO[33]; it was therefore probable that the diffusing substance detected optically was also Mg. The form of the absorbing defect was then postulated to be an Fe^{+3} ion coupled with a Mg^{+2} vacancy.

4. Substantial evidence was found that the visible region of the spectrum also contained optical structure probably due to impurities. This observation together with the fact that the interpretation of the behaviour of the ultraviolet bands was based on impurity reactions strongly suggest that most if not all the optical structure in the wavelength range investigated was due to impurities rather than color centers analogous to those in the alkali halides.

5. The introduction of the defect centers into the MgO crystals appeared to result in the development of a lattice stress.

6. Calculations of the diffusion coefficient based on the proposed mechanism indicated that both the 5.75 and the 4.40 eV peak were caused by the same defect and were involved in the same diffusion process. This process could be represented by:

$$D = 1.7 \times 10^5 \, e^{\frac{-77,000}{RT}}$$

over the temperature range 800 - 1100° C.

7. The 5.0 eV peak was also found to follow a diffusion relation; however, no conclusions were drawn concerning its form or its associated impurity.

VI. RECOMMENDATIONS FOR FURTHER WORK

It is now extremely doubtful from the results of this and other investigations that any color centers of a type similar to those in the alkali halides are present in any quantity in magnesium oxide. However, some methods used in studying the alkali halide coloring phenomena could be applied to magnesium oxide. For instance, it would be interesting to see if the vacancies generated by plastic deformation could produce an enhancement of both oxygen and X-ray colorability.

The nature of the defects causing all the peaks has not been determined. Both the 5.0 eV peak and the 2.3 eV peak (the latter due to X-irradiation only) have not been studied adequately. Moreover, the visible as-received optical structure observed provides another region of investigation. It is also evident that further work could be conducted using the spectra of aqueous solutions of various elements and correlating the results to the behaviour of impurities in solids such as MgO (similar to the work of Morin[38] using pure transition metal oxides and Moulson and Roberts[28] for water in silica glass).

There are three other regions of investigation suggested by this project. First, an adequate explanation of the stress pattern in Figure 13. has not been achieved. Secondly, the mechanism proposed should be verified using wider ranges of temperature, pressure and composition. The third region is the probable application of the technique used to other diffusing elements or substances; however, this technique appears to be useful only for fast diffusion rates. The quantitative analysis of those elements in MgO possessing visible peaks (for example, chromium) by optical density measurements appears to also be a useful technique to develop.

More closely related to metal-ceramic bonding could be a project concerned with the bonding properties of low melting-point metals when the optical absorption bands are present or absent and with variable amounts of impurities such as chromium, iron and manganese in the magnesium oxide. Low temperatures would be necessary, of course, to counter the effect of the vacuum annealing of the optical structure; these temperatures would ppssibly be less than 600° C. and certainly less than 800° C.

VII. BIBLIOGRAPHY

1. Seitz, F., Rev. Mod. Phys. 18, 384, (1948).
2. Seitz, F., Rev. Mod. Phys. 26, 7, (1954).
3. Hibben, J. H., Phys. Rev. 51, 530, (L) (1937).
4. Molnar, I. P and Hartmann, C. D., Phys. Rev. 79, 1015 (L) (1950).
5. Weber, H, Z. Physk. 130, 392, (1951).
6. Yamaka, E and Sawamoto, K., Phys. Rev. 101, 565, (1956).
7. Day, H. R., Phys. Rev. 91, 822, (1953).
8. Peria, W. T., Phys. Rev. 112, 423 (1953).
9. Shatas, R. A., Pomerantz, M. A., Marshall, J. F.,Phys. Rev. 109, 1953, (1958).
10. Marshall, J. F., Pomerantz, M. A., Shatas, R. A., Phys. Rev, 106, 423, (1957).
11. Yamashita, J., Phys. Rev. 111, 733, (1958).
12. Soshea, R. W., Dekker, A. J., and Sturtz, J. P., J. Phys. Chem. Solids, 5-6, 23, (1958).
13. Clarke, F. P., Phil. Mag. 2, (8), 607, (1957).
14. Johnson, P. D., Phys. Rev., 94, 845, (1954).
15. Reilling, G. H., and Hensley, E. B., Phys. Rev. 112, 1106, (1958).
16. Gandy, N. W., Phys. Rev. 111, 764, (1958).
17. Hansler, R. L. and Segelken, W. G., J. Phys. Chem. Solids, 13, 124, (1960).
18. Wertz, J. E., Auzins, P., Griffiths, J. H. E., and Orton, J. W., Disc. Fara. Soc. "Crystal Imperfections and the Chemical Reactivity of Solids", Aberdeen Univ. Press, Aberdeen, (1959).
19. Wertz, J. E. and Auzins, P., Phys. Rev. 106, 484, (1957).
20. Low, W., Phys. Rev. 105, 801, (1957).
21. Low, W., Phys. Rev. 105, 793, (1957).
22. Shepherd, W. G., Wright Air Development Center Technical Report, 57-760, August 1958.
23. Yamaka, E., Phys. Rev. 96, 293, (1954).
24. Kröger, F. A. and Vink, H. J., "Solid State Physics", Ed. F. Seitz and and D. Turnbull, Vol. 3, Academic Press (1956).
25. Hasselman, D. P. H., M.A.Sc. Thesis. University of British Columbia, (1959).

26. Clarke, J. F., M.A.Sc. Thesis, University of British Columbia (1960).

27. De Cleene, M. L. A., M.A.Sc. Thesis, University of British Columbia, (1961).

28. Moulson, A. J and Roberts, J. P., Nature 182, 200 (1958); Trans. British Cer. Soc. 59, 388, (1960).

29. Lothian, G. F., "Absorption Spectrophotometry", Hilger and Watts, London, (1959).

30. Prutton, C. F. and Maron, S. M., "Fundamental Principles of Physical Chemistry", MacMillan, New York, (1955).

31. Crank, J., "Mathematics of Diffusion", Clarendon Press, Oxford, (1951).

32. Barrer, R. M., "Diffusion in an Through Solids", University Press, Cambridge, (1951).

33. Lindner, R. and Parfitt, G. D., J. Phys. Chem. 26, 182, (1957).

34. See Schwab, G. M., Second International Congress of Surface Activity, II 230, (1957).

35. Winter, E. R. S., J. Chem. Soc., 1522, (1954).

36. (Mrs.) A. M. Armstrong, Private Communication.

37. Lan-Ying Lin as quoted by Pratt, P. L., "Vacancies and other Point Defects in Metals and Alloys", Institute of Metals Monograph No. 23 London (1958).

38. Morin, F. J., "Semiconductors", (ed. N. B. Hannay) Rheinhold, New York (1959).

39. Brownlee, K. A., "Industrial Experimentation", Her Majesty's Stationery Office, London (1949).

40. Fisher, R. A., "Statistical Methods for Research Workers", Oliver and Boyd, Edinburgh (1954).

III. APPENDICES

APPENDIX A

Spectrochemical Analysis of MgO (Condensed from letters from John H. Kelly, The Steel Company of Canada)

An arc chamber was constructed using a special glass envelope material. The gas mixture used to obtain the desired arc characteristics was 50% argon and 50% oxygen. The transmittance of each of eleven spectral lines and their background was measured in duplicate on each of eleven samples and five standards; the standard was reagent-grade MgO. In addition, emulsion calibration was performed for each wave-length region.

The most important limitation of the technique was that the electrodes were not water-cooled. This prevented the use of arc currents of greater than about 5 amperes and exposures longer than 30 seconds. The sample size was therefore kept to 7 mgs; this size did not lend itself to good sampling procedures. Moreover, the accuracy of the results were difficult to determine since the addition standards were of a heterogeneous nature.

APPENDIX B

Results of Heating in Oxygen

(Crystal 14, 4.40 and 5.75 eV Peaks.)

TABLE I

Specimen: 14 P_2
Temperature 1102 ±5° C.

d_A X 10^3		100% corr'tn		Δd_t X 10^3		Visible corr'tn	Δd_t X 10^3		Time	(Time)$^{1/2}$
4.40	5.75	4.40	5.75	4.40	5.75		4.40	5.75	min.	
564	1135	0.942	1.0	344	815	11	333	804	30	5.48
642	1308	0.942	1.0	422	988	21	401	967	45	6.71
695	1428	0.942	1.0	475	1108	19	456	1089	60	7.74
799	1668	0.940	0.993	550	1351	38	512	1313	90	9.47
828	1748	0.940	1.0	598	1428	22	576	1406	105	10.23
884	1772	0.944	1.0	663	1452	35	628	1417	137	11.70
907	1878	0.944	1.0	686	1558	41	645	1517	167	12.91
922	1993	0.940	1.0	793	1673	36	667	1637	207	14.38
933	-	0.939	-	715	-	32	688	-	267	16.33
950	2089	0.933	1.0	735	1769	42	693	1727	327	18.08
940	2000	0.948	1.005	717	1682	42	675	1640	387	19.67
940	1913	0.940	1.0	720	1593	41	679	1552	447	21.10
948	2045	0.948	1.0	725	1725	40	685	1685	497	22.30
958	2091	0.941	1.0	739	1771	44	695	1727	578	24.00
971	1969	0.944	1.003	751	1649	47	704	1602	625	25.00
989	2043	0.942	0.997	769	1723	64	705	1659	656	25.60

d_M X 10^3

visible 261
282.5 246
216 320

average
Δd_s X 10^3 at 4.40 eV = 687
Δd_s X 10^3 at 5.75 eV = 1654

TABLE II

Specimen: 14 J
Temperature 1082° C. ± 6

469	987	0.937	1.0	286	673	5	281	668	30	5.48
608	1286	0.942	1.0	423	972	12	411	960	60	7.75
676	1420	0.947	1.0	488	1106	24	464	1082	75	8.66
719	1499	0.942	1.0	534	1185	21	513	1164	90	9.48
765	1590	0.950	1.0	576	1276	22	554	1254	105	10.25
822	1678	0.942	1.0	637	1346	38	599	1308	120	10.94
886	1998	0.942	1.0	701	1484	51	650	1433	135	11.61
924	1821	0.941	1.0	740	1507	52	688	1455	150	12.24
966	1986	0.948	1.0	778	1672	58	720	1614	165	12.84
993	-	0.943	-	808	-	56	752	-	180	13.42
1034	-	0.945	-	847	-	32	815	-	210	14.50
1066	-	0.945	-	880	-	28	852	-	240	15.48
1133	-	0.941	-	949	-	35	914	-	271	16.43
1209	-	0.942	-	1025	-	78	947	-	301	17.34
1243	-	0.944	-	1057	-	73	984	-	340	18.43
1307	-	0.944	-	1121	-	74	1047	-	410	20.25

d_M X 10^3 - 350 mμ = 225; 282.5 = 211; 216 = 314.

TABLE III

Specimen: 14 M
Temperature 1045°C. ±5

d_A X 10^3		100% corr'tn		Δd_t X 10^3		Visible corr'tn	Δd_t X 10^3		Time	$(\text{Time})^{1/2}$
4.40	5.75	4.40	5.75	4.40	5.75		4.40	5.75	min.	
366	712	.937	1.0	208	493	11	197	482	30	5.48
432	871	.942	1.0	272	654	-1	273	653	60	7.75
471	950	.947	1.0	309	731	7	302	724	75	8.66
506	1018	.942	1.0	346	799	5	341	794	90	9.48
532	1081	.948	1.0	369	862	13	356	849	105	10.25
558	1137	.939	1.0	400	918	15	385	903	120	10.94
585	1194	.939	1.0	426	975	15	411	960	135	11.61
635	1282	.941	1.0	475	1063	33	442	1030	150	12.24
650	1336	.946	1.0	489	1117	26	463	1091	165	12.84
673	1367	.941	1.0	514	1148	31	483	1117	180	13.42
633	-	.942	-	474	-	-11	485	48 hrs. at RT		
692	1433	.943	1.0	531	1214	6	525	1208	210	14.50
707	1493	.942	1.0	537	1274	-2	539	1276	240	15.48
717	1502	.942	1.0	558	1283	3	555	1280	16 hrs. at RT	
748	1563	.940	1.0	589	1344	16	573	1328	271	16.43
804	1671	.941	1.0	645	1452	50	595	1402	301	17.34
829	1725	.942	1.0	670	1506	59	611	1447	340	18.43
829	-	.941	-	670	-	58	612	65 hrs. at RT		
863	1882	.944	1.0	700	1663	61	641	1602	410	20.25
855	1814	.944	1.0	695	1595	55	640	1540	470	21.70
863	1765	.943	1.0	703	1546	65	638	1481	525	22.90
874	1812	.943	1.0	714	1593	67	647	1526	555	23.50
897	1876	.938	.994	739	1660	72	667	1588	590	24.30
897	-	.937	-	739	-	73	666	-	"	"

d_M X 10^3

350 mμ	208
282.5	186
216	219

Δd_s X 10^3 at 4.40 eV = .638 avg.
Δd_s X 10^3 at 5.75 eV = 1600 avg.

Note: RT = Room temperature.

TABLE IV

Specimen: 14 Q
Temperature 994 ± 4° C.

d_A X 10^3		100% corr'tn		Δd_t X 10^3		Visible corr'tn	Δd_t X 10^3		Time	
4.40	5.75	4.40	5.75	4.40	5.75		4.40	5.75	hrs ~~min~~.	(Time) $^{1/2}$
326	584	.942	1.0	114	260	5	109	255	0.5	.707
397	772	.944	1.0	184	448	-2	186	450	1.5	1.224
580	1202	.942	1.0	367	878	5	362	873	5.5	2.345
666	1419	.940	1.0	454	1095	11	443	1084	8.0	2.83
764	1663	.935	0.995	554	1341	11	543	1330	11.5	3.39
774	1682	.950	1.0	558	1356	7	551	1349	12.5	3.53
843	1850	.950	1.0	626	1526	15	611	1511	15.0	3.87
906	2000	.942	1.0	694	1676	11	685	1665	20.0	4.47
953	2055	.948	1.0	737	1731	15	722	1716	37.1	6.09
957	2003	.946	0.984	742	1679	15	727	1664	39.5	6.28
978	2003	.942	0.984	765	1679	32	733	1647	41.5	6.44
988	2125	.942	1.0	776	1801	26	750	1775	58.5	7.65
1008	2068	.938	0.984	797	1744	40	757	1704	61.0	7.81
999	2244	.943	1.0	785	1929	32	753	1888	63.0	7.93
1016	2143	.943	1.0	802	1819	34	768	1785	67.0	8.18

d_M X 10^3	
350 mμ	248
282.5	239
216	324

average
Δd_s X 10^3 at 4.40eV = 757
Δd_s X 10^3 at 5.75eV = 1788

TABLE V

Specimen: 14 N
Temperature 982 ± 6

d_A X 10^3		100% corr'tn		Δd_t X 10^3		Visible corr'tn	Δd_t X 10^3		Time (Time)	$t_{1/2}$
4.40	5.75	4.40	5.75	4.40	5.75		4.40	5.75	hrs mins.	
310	671	.950	1.014	145	368	9	136	359	1.0	1.00
366	787	.935	1.000	208	491	14	194	477	2.0	1.42
411	906	.941	1.000	250	610	9	241	609	3.0	1.73
462	1000	.935	1.000	350	704	19	286	685	4.0	2.00
524	1124	.937	1.000	366	828	32	334	796	5.0	2.24
516	1109	.942	1.000	355	813	25	330	788	24 hrs.	RT
564	1190	.942	1.000	403	894	42	361	852	6.0	2.45
601	1253	.940	1.000	441	957	47	394	910	7.0	2.65
648	1356	.940	1.000	489	1060	54	435	1006	8.0	2.83
667	1402	.940	1.000	507	1106	49	458	1057	9.0	3.00
710	1523	.940	1.000	550	1227	61	489	1166	10.0	3.16
727	1507	.937	1.000	569	1211	65	504	1146	11.0	3.32
762	1582	.940	1.0	602	1386	71	531	1215	12.0	3.46
759	-	.944	-	598	-	60	538	-	72 hrs.	RT
878	1952	.940	1.0	719	1656	120	599	1536	13.5	3.67
872	1873	.943	1.0	711	1577	96	615	1481	14.5	3.81

d_M X 10^3 - 350 mμ = 203; 282 = 187; 216 = 296.

TABLE VI

Specimen: 14 D
Temperature 959 ± 4°C.

373	822	.927	.990	145	374	5	140	369	2.0	1.42
432	983	.950	1.014	192	524	-4	196	528	4.0	2.00
473	1034	.935	1.0	240	681	16	224	565	5.0	2.24
499	1098	.941	1.0	264	645	15	249	630	6.0	2.45
537	1133	.935	1.0	305	714	29	276	685	7.0	2.65
553	1178	.937	1.0	319	759	19	300	740	8.0	2.83
553	1169	.942	1.0	317	750	14	303	736	24 hrs.	RT
573	1213	.942	1.0	337	794	15	322	779	9.0	3.00
623	1285	.940	1.0	388	866	40	348	826	10.0	3.16
643	1325	.940	1.0	409	906	34	375	872	11.0	3.32
678	1374	.940	1.0	439	955	37	402	918	12.0	3.46
710	1468	.939	1.0	475	1049	47	428	1002	13.0	3.61
753	1524	.939	1.0	520	1105	70	450	1035	14.0	3.74
767	1524	.940	1.0	532	1105	63	469	1042	15.0	3.87
763	-	.944	-	527	-	68	459	-	22 hrs.	RT
812	1702	.940	1.0	577	1283	60	517	1223	16.5	4.06
832	1723	.943	1.0	596	1304	74	522	1230	17.5	4.19

d_M X 10^3

350 mμ	273	214	453
282.5	262	216	419

TABLE VII

Specimen: 14 L
Temperature 946 ± 4° C.

d_A X 10^3		100% Corr'tn		Δd_t X 10^3		Visible corr'tn	Δd_t X 10^3		Time	(Time)$^{1/2}$
4.36	5.81	4.36	5.81	4.36	5.81		4.36	5.81	hr.	
299	605	.942	1.01	101	244	5	96	239	1.0	1.00
343	711	.935	1.0	147	354	18	129	336	2.0	1.42
372	792	.930	1.0	178	435	12	166	423	3.0	1.73
392	850	.934	1.0	196	493	11	185	482	4.0	2.00
429	930	.933	1.0	234	573	22	212	551	5.0	2.24
431	956	.937	1.0	235	599	3	232	596	6.0	2.45
464	1011	.939	1.0	267	654	17	250	637	7.0	2.65
511	1100	.943	1.0	311	743	42	269	701	8.0	2.83
509	1120	.940	1.01	311	760	24	287	736	9.0	3.00
528	1154	.942	1.0	330	797	28	302	760	10.0	3.16
540	1197	.936	1.0	344	840	27	317	813	11.0	3.32

d_M X 10^3

350 mμ	236
285	225
214	357

TABLE VIII

Specimen: 14 C
Temperature 906 ± 3° C.

4.40	5.75	4.40	5.75	4.40	5.75		4.40	5.81		
236	500	.925	0.992	93	222	5	88	217	2.0	1.42
267	583	.937	1.0	118	302	1	117	301	4.0	2.00
293	606	.930	1.0	147	325	2	145	323	6.0	2.45
496	1085	.935	1.0	349	804	30	319	774	24.0	4.90
500	1126	.937	0.990	352	849	13	339	836	28.5	5.34
598	1319	.940	1.0	448	1038	14	434	1024	44.5	6.67
627	1374	.940	1.0	476	1093	20	456	1073	46.5	6.82
620	1368	.942	0.994	469	1089	18	451	1071	48.5	6.97
722	1624	.931	0.994	578	1346	29	549	1317	67.5	8.21
729	1629	.930	0.990	584	1352	24	560	1328	71.0	8.42
825	1720	.934	0.990	678	1443	43	635	1400	89.0	9.43
896	2065	.930	0.990	751	1788	46	705	1742	117.5	10.84
962	2252	.940	1.0	812	1971	49	763	1922	134.5	11.60
967	2310	.940	1.0	812	2029	47	770	1972	137.5	11.72

d_M X 10^3

350 mμ	197
282.5	177
216	281

TABLE IX

Specimen: 14 E
Temperature 842 ± 7° C.

d_A X 10^3		100% Corr'tn		Δd_t X 10^3		Visible corr'tn	Δd_t X 10^3		Time	(Time)$^{1/2}$
4.43	5.75	4.43	5.75	4.43	5.75		4.43	5.75	hr.	
392	681	.928	.986	41	93	4	37	89	2.0	1.42
435	787	.938	1.0	79	192	6	73	186	9.0	3.00
503	926	.942	1.0	145	331	35	110	296	22.2	4.71
507	-	.942	-	150	-	38	112	28	hrs. at RT	
556	1069	.933	1.0	203	474	38	165	436	44.2	6.65
531	971	.943	1.0	173	376	46	127	330	28.2	5.31
641	1256	.942	1.0	284	661	49	235	612	91.2	9.55
665	1321	.942	1.0	307	726	42	265	684	114.7	10.70
732	1524	.941	.990	375	934	63	312	871	137.7	11.73
733	1454	.938	.990	377	863	62	315	801	149.0	12.20
756	1500	.940	.990	399	909	58	341	841	159.0	12.60
800	1637	.945	1.0	440	1042	72	368	970	183.0	13.52
798	1583	.942	1.0	440	988	71	369	917	187.0	13.67
850	1763	.945	1.0	491	1168	96	395	1072	206.0	14.30
930	1960	.941	1.0	574	1365	123	451	1242	251.5	15.85

d_M X 10^3

350 mμ	389
280	384
216	595

TABLE X

Specimen: 14 B
Temperature 792 ± 4° C.

4.49	5.80	4.49	5.80	4.49	5.80		4.49	5.80		
289	591	.933	1.0	14	54	0	14	54	2.0	1.42
295	643	.933	1.0	21	106	0	21	106	6.5	2.55
329	713	.942	1.0	50	176	15	35	161	24.5	4.95
339	732	.940	1.0	60	195	22	38	173	29.0	5.39
365	781	.943	1.0	86	244	26	60	218	45.0	6.70
380	808	.943	1.0	105	271	35	70	236	50.5	7.15
430	882	.935	1.0	153	345	53	100	292	69.0	8.30
423	886	.932	1.0	150	349	49	101	300	72.5	8.52
419	879	.941	1.0	137	342	33	104	309	90.5	9.52
447	927	.940	1.0	170	390	43	127	347	119.0	10.90
450	942	.941	1.0	173	405	41	132	364	136.0	11.66
464	976	.942	1.0	185	430	50	135	380	139.0	11.80

d_M X 10^3

350 mμ	298
277	305
214	537

APPENDIX C

Results of Heating in Air

(Crystal 5; 4.40 and 5.75 eV Peaks)

TABLE I

Specimen: 5 D 2
Temperature 1094 ± 5°C.

d_A X 10^3		100% corr'tn		Δd_t X 10^3		Visible corr'tn	Δd_t X 10^3		Time min.	$(\text{Time})^{\frac{1}{2}}$
4.36	5.75	4.36	5.75	4.36	5.75		4.36	5.75		
353	684	.945	1.0	196	472	16	180	456	15	3.87
452	899	.943	1.0	297	687	29	268	658	30	5.48
508	1017	.942	1.0	353	805	30	323	775	46	6.78
569	1649	.940	1.0	415	937	38	377	899	61	7.81
619	1264	.943	1.0	463	1052	45	418	1007	77	8.77
675	1375	.941	1.0	520	1163	53	467	1110	92	9.58
740	1542	.943	1.0	584	1330	48	536	1282	124	11.13
858	1805	.952	1.0	702	1593	75	627	1578	166	12.88
893	1918	.940	1.0	737	1706	69	668	1637	201	14.18
949	1984	.941	1.0	793	1772	86	707	1686	224	14.98
999	-	.943	1.0	844	1888	92	752	1796	264	16.25
1041	-	.943	0.98	884	1984	98	786	1886	311	17.62
1072	-	.943	0.974	916	2007	101	815	1906	371	19.25
1096	-	.942	0.978	940	2065	111	829	1954	431	20.75
1105	-	.946	0.98	947	2107	106	841	2001	491	22.15
1126	-	.941	0.968	971	2016	119	852	1997	537	23.15
1169	-	.943	1.007	1013	2763	136	877	2627	597	24.40
1167	-	.943	0.992	1011	2212	128	883	2084	657	25.60
1191	-	.941	0.992	1035	2394	143	892	2251	745	27.30
1196	-	.950	0.980	1037	2218	137	900	2081	865	29.40
1208	-	.945	0.990	1051	2315	143	908	2172	1090	33.00
1210	-	.937	-	1056	-	148	908	-	Repeat	

d_M X 10^3	
350 mμ	204
285	182
216	212

average

Δd_s X 10 at 5.75 eV = 2130
Δd_s X 10 at 4.40 eV = 908

TABLE II

Specimen: 5 C 2
Temperature 1094 ± 5° C.

d_A X 10^3		100% Corr'tn		Δd_t X 10^3		Visible corr'tn	Δd_t X 10^3		Time min.	$(\text{Time})^{\frac{1}{2}}$
4.36	5.75	4.36	5.75	4.36	5.75		4.36	5.75		
397	718	.945	1.0	223	505	27	196	478	15	3.78
457	863	.943	1.0	275	650	25	250	625	30	5.48
532	1018	.942	1.0	360	805	35	325	770	46	6.78
597	1153	.940	1.0	426	940	49	377	891	61	7.81
650	1270	.942	1.0	478	1057	58	420	999	77	8.77
696	1363	.941	1.0	525	1150	63	462	1087	92	9.58
828	1611	.940	1.0	658	1398	114	544	1284	124	11.13
873	1722	.942	1.0	702	1509	113	589	1396	166	12.88
899	1777	.942	1.0	727	1564	114	613	1450	201	14.16
930	1809	.941	1.0	797	1596	137	622	1459	224	14.98
939	1803	.943	1.0	766	1590	134	632	1456	264	16.25
943	1848	.942	1.0	772	1635	145	627	1490	311	17.62
996	1918	.943	1.0	823	1705	156	657	1549	371	19.25
1023	1949	.942	1.0	851	1736	179	672	1557	431	20.75
1039	-	.946	0.980	865	1791	179	686	1612	491	22.15
1065	-	.941	0.970	893	1791	190	703	1601	537	23.15
1093	-	.944	1.013	921	1791	190	712	1808	597	24.40
1051	-	.943	0.997	879	1819	194	685	1625	657	25.60
1060	-	.941	0.980	889	1796	192	693	1600	745	27.30

	d_M X 10^3	
350 mμ	220	
285.0	198	
216	213	

average

Δd_s X 10 at 5.75 eV = 1600
Δd_s X 10 at 4.40 eV = 690

TABLE III

Specimen: 5 A 3
Temperature 1060° C. ± 10

d_A		100% Corr'tn		Δd_t X 10^3		Visible corr'tn Δd_t X 10^3			Time	
4.42	5.69	4.42	5.69	4.42	5.69		4.42	5.69	~~min.~~ hrs	$(\text{Time})^{1/2}$
0.657	1.25	.940	1.0	462	937	49	413	924	2.0	1.42
0.764	1.65	.933	1.0	572	1298	64	508	1234	3.0	1.73
0.854	1.697	.939	1.004	660	1329	76	584	1269	4.0	2.00
0.963	2.143	.942	1.006	767	1788	84	683	1704	5.0	2.24
0.967	2.017	.938	1.0	773	1665	86	687	1579	18 hrs at RT	
1.119	-	.938	-	925	--	140	785	-	6.0	2.45
1.135	-	.941	-	940	-	107	833	-	7.0	2.64
1.173	-	.941	-	978	-	105	873	-	8.0	2.83
1.263	-	.940	-	1069	-	135	933	-	9.0	3.00
1.407	-	.918	-	1226	-	156	1070	-	11.0	3.32
1.504	-	.939	-	1309	-	159	1150	-	12.5	3.53

d_M X 10^3

350 mμ	213
281	222
218	352

TABLE IV

Specimen:5 E
Temperature 1004 ± 10° C.

d_A X 10^3

4.37	5.69	4.37	5.69	4.37	5.69		4.37	5.69	Hrs.	
374	738	.930	1.0	248	542	43	205	499	2.0	1.42
418	847	.940	1.0	277	651	36	241	615	3.0	1.73
467	950	.928	0.995	342	757	47	295	710	4.0	2.00
522	1054	.935	1.0	393	858	39	354	819	5.5	2.34
541	1115	.940	1.011	409	915	49	360	866	18 hrs at RT	
622	1230	.929	0.993	496	1038	60	436	978	7.0	2.64
646	1317	.930	0.995	520	1124	64	458	1060	8.0	2.83
713	1425	.930	0.995	586	1232	67	519	1165	10.0	3.16
760	1602	.934	1.0	632	1406	59	573	1247	12.0	3.46
934	2000	.927	0.993	810	1986	103	707	1687	16.0	4.00

d_M X 10^3

350 mμ	170
284	158
218	196

TABLE V

Specimen: 5 C 1
Temperature 996° C. ± 8

$d_R \times 10^3$ 4.40	5.75	100% Corr'tn 4.40	5.75	$d_t \times 10^3$ 4.40	5.75	Visible corr'tn	$d_t \times 10^3$ 4.40	5.75	Time hrs.	$(\text{Time})^{1/2}$
358	659	.942	1.0	183	430	15	168	415	2.0	1.42
470	890	.943	1.0	294	661	35	259	626	4.0	2.00
598	1069	.943	1.0	422	851	41	381	810	6.0	2.45
645	1203	.943	1.0	470	974	51	419	923	8.0	2.83
862	1691	.946	1.0	686	1462	56	630	1406	26.0	5.10
928	1804	.941	1.0	754	1575	83	671	1492	58.0	7.61
960	1841	.945	1.0	784	1622	99	685	1523	72.0	8.48
982	1876	.946	1.0	806	1647	108	698	1539	78.0	8.83
1023	1907	.945	1.0	847	1678	122	725	1556	94.0	9.69
1018	1940	.942	1.0	843	1711	122	721	1589	100.0	10.00
1063	-	.946	1.0	887	1896	122	765	1769	117.0	10.80
1115	-	.952	0.986	936	1854	152	784	1702	123.0	11.10
1088	-	.950	1.01	910	1910	102	808	1808	139.0	11.79
1142	-	.950	-	963	1960	134	829	1826	140.0	11.82
1136	-	.937	0.986	963	1957	132	831	1819	repeat	
1177	-	.948	1.01	999	2085	148	841	1937	157.0	12.51
1218	-	.950	1.0	1039	2038	150	889	1888	179.0	13.38
1270	-	.945	1.012	1094	2302	168	926	2134	201.0	14.14
1270	-	.950	0.975	1091	1937	143	948	1794	220.0	14.83
1270	-	.953	1.0	1090	2202	151	939	2050	Repeat	
1396	-	.950	-	1217	-	197	1020	-	249.0	15.80
1387	-	.948	-	1209	-	187	1022	-	270.0	16.43
1470	-	.947	-	1292	-	192	1100	-	313.0	17.70
1453	-	.941	-	1279	-	197	1082	-	"	"
1431	-	.941	-	1257	-	166	1091	-	"	"
1497	-	.945	-	1321	-	184	1142	-	336.0	18.30
1494	-	.945	-	1318	-	187	1131	-	383.0	19.58

$d_M \times 10^3$	
350 mμ	219
282.5	201
216	229
218	218

average

$\Delta d_s \times 10^3$ at 5.75 eV = 1600
$\Delta d_s \times 10^3$ at 4.40 eV = 720

TABLE VI

Specimen: 5 A 2
Temperature 996 ± 10° C.

d_A X 10^3 4.36	5.75	100% Corr'tn 4.36	5.75	Δd_t X 10^3 4.36	5.75	Visible corr'tn	Δd_t X 10^3 4.40	5.75	Time hrs.	(Time) ½
293	558	.935	1.0	166	336	50	110	286	2.0	1.42
333	647	.934	1.0	208	442	46	162	396	4.0	2.00
603	1333	.940	1.0	474	1111	46	428	1065	22.0	4.69
629	1377	.936	1.0	502	1155	60	442	1095	23.0	4.79
880	2229	.937	1.0	753	2007	83	670	1924	68.0	8.25
883	-	.935	-	755	-	75	680	-	73.5	8.57
998	-	.930	-	874	-	107	767	-	89.0	9.43

d_M X 10^3	
350 mμ	167
285	155
216	222

TABLE VII

Specimen: 5 A 1
Temperature 940° C. ± 7

4.42	5.75	4.42	5.75	4.42	5.75		4.42	5.75		
270	492	.938	1.0	48	200	0	48	200	2.0	1.42
329	630	.939	1.0	133	320	3	130	317	4.0	2.00
374	712	.939	1.0	181	420	3	198	417	7.5	2.74
408	797	.940	1.0	213	485	0	213	485	9.0	3.00
539	1033	.937	1.0	345	741	-5	350	746	20.5	4.53
712	1382	.935	1.006	519	1090	11	508	1079	43.5	6.59
719	1420	.943	1.0	517	1128	3	514	1125	44.5	6.67
996	2229	.940	1.0	808	1937	24	784	1913	89.5	9.46
1104	2620	.939	0.995	909	2329	29	880	2300	95.0	9.75
1219	-	.936	-	1025	-	33	992	-	110.5	10.50
				397	871	-3	400	874	26.5	5.15

d_M X 10^3	
350 mμ	237
281	222
216	292
214	310

TABLE VIII

Specimen: 5 H 1
Temperature 909 ± 9° C.

d_A X 10^3 4.43	5.7	100% corr'tn 4.43	5.7	Δd_t X 10^3 4.43	5.7	Visible corr'tn	Δd_t X 10^3 4.43	5.7	Time hrs.	(Time)$^{1/2}$
329	443	.940	1.0	109	181	6	103	175	2.5	1.58
383	568	.940	1.0	164	306	7	157	299	7.5	2.74
577	908	.907	0.945	374	671	85	289	586	34.5	5.87
565	921	.935	0.970	348	676	18	333	661	38.0	6.17

Specimen Broke

d_M X 10^3	
350 mμ	230
280	246
218	262

TABLE IX

Specimen: 5 J
Temperature 909 ± 7.C.

465	798	.930	0.990	294	562	82	212	480	2.0	1.42
465	812	.943	1.0	297	571	72	225	499	4.0	2.00
462	788	.942	1.0	286	547	50	236	497	6.0	2.45
592	1040	.940	1.0	417	799	67	350	732	25.0	5.00
611	1088	.940	0.990	435	852	69	366	783	29.5	5.43
666	1168	.942	1.0	489	927	73	416	854	45.5	6.74
671	1168	.942	1.0	494	927	76	418	851	47.5	6.88
689	1203	.934	0.994	576	965	87	429	878	49.5	7.03
750	1340	.935	0.995	576	1096	79	497	1017	68.5	8.27
764	1363	.932	0.990	592	1128	84	508	1044	72.0	8.49
843	1421	.943	0.990	665	1285	95	570	1190	90.0	9.49
929	1751	.940	0.980	752	1514	107	645	1407	118.5	10.88
964	1802	.950	1.0	787	1561	98	689	1463	135.5	11.63
983	1915	.942	1.0	806	1674	96	710	1518	138.5	11.78

d_M X 10^3	
350 mμ	215
280	203
218	241

TABLE X

Specimen: 5 B
Temperature 850 ± 10 °C.

d_A X 10^3 4.36	5.69	100% 4.36	Corr'tn 5.69	Δd_t X 10^3 4.36	5.69	Visible corr'tn	Δd_t X 10^3 4.36	5.69	Time hrs.	$(\text{Time})^{\frac{1}{2}}$
269	380	.937	1.0	71	106	56	15	50	2.0	1.42
289	426	.939	1.006	90	150	57	33	93	6.5	2.55
334	542	.937	1.0	137	258	61	76	197	23.5	4.85
334	537	.939	1.006	136	276	52	84	224	29.0	5.38
341	570	.935	1.0	144	296	53	91	243	33.0	5.74
363	606	.940	1.0	164	332	57	107	275	44.0	6.63
379	639	.935	1.0	183	365	58	125	307	50.0	7.07
409	701	.937	0.993	211	430	64	147	366	68.0	8.25
404	713	.932	0.995	209	441	58	151	383	73.0	8.55
478	863	.940	1.05	279	587	58	221	529	137.0	11.70

d_M X 10^3	
350 mμ	238
285	226
218	274

TABLE XI

Specimen: 5 J
Temperature 795 ± 7 °C.

4.52		4.52		4.52			4.52			
248	337	.943	1.0	62	96	56	6	40	5.5	2.35
283	417	.940	1.0	108	176	68	40	108	21.0	4.58
336	510	.905	0.945	187	294	91	96	203	95.0	9.75
312	507	.938	1.0	137	266	52	87	214	117.0	10.80
325	519	.941	1.010	148	273	58	90	215	121.5	11.02
344	563	.943	1.0	167	322	51	116	271	162.5	12.74
353	587	.940	1.0	177	346	54	123	292	186.5	13.65
353	593	.940	1.0	177	352	51	126	301	191.5	13.83
374	610	.925	0.996	203	371	70	133	301	207.5	14.40
374	629	.940	1.0	198	388	59	139	329	214.5	14.65
413	680	.933	1.0	240	439	84	156	355	230.5	15.20
418	698	.933	0.992	245	461	81	164	380	254.0	15.93
442	730	.938	0.997	268	489	86	182	403	277.5	16.65
448	763	.950	1.010	268	518	77	191	441	325.5	18.05

d_M X 10^3	
350 mμ	215
280	203
218	241

APPENDIX D

Results of Spectra Analyses

TABLE I

Specimen: 14 P 2
Temperature 1102° C.

Data: Log Δd_t Vs. $(\Delta E)^2$ 5.75 eV Peak

E eV	$(\Delta E)^2$	Δd_t X 10^3 30	45	327
5.3	0.203	520	619	1127
5.4	0.123	603	718	1309
5.5	0.063	679	818	1514
5.6	0.023	791	954	1711
5.75	0	804	977	1724

Data: Log Δd_t Vs. $(\Delta E)^2$ 4.40 eV Peak

Time mins.	Δd_t X 10^3 4.40	5.75	4.4	Δd_t X 10^3 4.3	4.2	4.1	4.0
30	333	11	322	314	278	211	140
45	401	14	387	372	326	243	154
327	693	24	669	660	589	456	302

Data: Δd_t Vs. $t^{\frac{1}{2}}$ 5.0 eV Peak

Time mins.	Δd_t X 10^3 obs'd	Δd_t X 10^3 4.4	5.75	Sum calc'd	Δd_t X 10^3 5.0
30	330	51	216	267	63
45	389	61	259	320	69
60	444	70	292	362	82
327	704	105	463	568	137
497	677	104	452	556	121
578	697	105	440	545	152
387	666	103	452	555	111
447	667	103	416	519	148
656	694	107	445	552	142

Δd_s X 10^3 5.0 eV Peak = 135 avg.

TABLE II

Data: Log Δd_t Vs. $(\Delta E)^2$ 5.75 eV Peak

Specimen: 14 J
Temperature 1082° C.

E eV	$(\Delta E)^2$	Δd_t X 10^3 30	65	70	105
5.3	.2025	438	631	729	843
5.4	.1225	504	727	838	975
5.5	.0625	567	821	943	1099
5.6	.0225	622	900	1027	1215
5.7	.0025	658	948	1076	1255
5.75	0	668	960	1082	1255

Peak occurs at 5.70 eV (150 min. only):

E	$(\Delta E)^2 \Delta d_t$ X 10^3
5.3	0.16 1045
5.4	0.09 1191
5.5	0.04 1330
5.6	0.01 1425
5.7	0.00 1458
5.75	0.0025 1455

Data: Log Δd_t Vs. $(\Delta E)^2$ 4.40 eV Peak

Time mins.	Δd_t X 10^3 4.40	5.75	4.4	Δd_t X 10^3 4.3	4.2	4.1	4.0
30	281	10	271	261	221	-	103
75	464	16	448	433	364	-	168
105	554	18	536	513	430	-	193
150	688	29	695	634	538	408	256

Data: Δd_t Vs $t^{\frac{1}{2}}$ 5.0 eV Peak

Time mins.	Δd_t X 10^3 obs'd	Δd_t 4.40	X 10^3 5.75	Sum calc'd	Δd_t X 10^3 5.0
30	276	36	181	217	59
60	397	53	260	313	84
75	459	59	293	352	107
90	494	66	317	383	111
105	534	71	342	413	121
120	576	77	356	433	143
135	634	84	389	473	161
150	668	88	468	556	112
165	699	93	438	531	168

TABLE III

Specimen: 14 M
Temperature 1045° C.

Data: Log Δd_t Vs. $(\Delta E)^2$ 5.75 eV Peak

E	$(\Delta E)^2$	Δd_t X 10^3 60	90	120
5.3	0.203	427	531	603
5.4	0.123	493	613	697
5.5	0.063	555	688	782
5.6	0.023	609	760	847
5.7	0.0025	644	786	895
5.75	0	654	794	903

Data: Log Δd_t Vs. $(\Delta E)^2$ 4.40 eV Peak

Time mins.	Δd_t X 10^3 4.40	5.75	Δd_t (E) X 10^3 4.4	4.3	4.2	4.1	4.0
60	273	12	261	255	221	171	107
90	341	15	326	322	280	220	143
120	385	17	368	359	309	238	152
30	197	9	188	corrected.			
75	302	14	288				
105	356	16	340				
135	411	18	393				
301	595	27	568				
340	611	28	583				
240	555	24	531				
271	573	25	548				

Data: Δd_t Vs. $t^{\frac{1}{2}}$ 5.0 eV Peak

Time mins.	Δd_t X 10^3 obs'd	Δd_t 4.4	X 10^3 5.75	Sum calc'd	Δd_t X 10^3 5.0
60	268	48	194	242	26
90	339	60	236	296	43
120	382	67	268	335	47
150	442	77	306	383	69
165	465	81	324	405	60
180	479	84	331	415	64
210	513	192	358	450	63
410	639	111	474	585	54
470	629	112	455	567	62
525	639	111	438	549	90
555	642	113	451	564	78
30	188	34	144	178	10
75	297	53	214	267	30
105	356	62	251	313	43
135	404	72	284	356	48
301	595	104	414	518	77
340	600	106	427	535	65
240	536	99	376	475	61
271	565	100	394	494	71

TABLE IV

Specimen: 14 Q
Temperature 996 ° C.

Data: $\text{Log}\Delta d_t$ Vs. $(\Delta E)^2$ 5.75 eV Peak

E eV	$(\Delta E)^2$	Δd_t X 10^3 0.5	5.5	8.0
5.3	0.203	165	580	705
5.4	0.123	194	667	816
5.5	0.063	222	754	921
5.6	0.023	240	821	1013
5.7	0.0025	245	858	1054
5.75	0	255	872	1083

Data: $\text{Log}\Delta d_t$ Vs. $(\Delta E)^2$ 4.40 eV Peak

Time hrs.	Δd_t X 10^3 4.4	5.75	Δd_t X 10^3 4.4	4.3	4.2	4.1	4.0
0.5	109	5	104	101	86	66	41
5.5	362	16	346	343	294	226	143
8.0	443	20	423	419	360	273	173

Data: Δd_t Vs. $t^{\frac{1}{2}}$ 5.0 eV Peak

Time hrs.	Δd_t X 10^3 obs'd	Δd_t X 10^3 4.4	5.75	Sum calc'd	Δd_t X 10^3 5.0
0.5	108	17	75	92	16
1.5	187	29	133	162	25
5.5	367	56	258	314	53
8.0	447	69	320	389	58
11.5	553	85	392	477	76
12.5	551	86	399	485	66
15.0	621	95	446	541	80
20.0	688	107	491	498	90
37.1	727	113	506	619	108
39.5	732	114	486	600	132
41.5	739	115	485	600	139
58.5	745	117	523	640	105
61.0	762	118	504	622	140
63.0	752	115	568	685	67
67.0	768	120	526	646	122

Δd_s X 10^3 5.0 eV avg.=124

TABLE V

Specimen: 14 N
Temperature 982° C.

Data: Log Δd_t Vs. $(\Delta E)^2$ 5.75 eV Peak

E eV	$(\Delta E)^2$	Δd_t X 10^3 2	4	6
5.3	0.203	314	480	592
5.4	0.123	377	546	675
5.5	0.063	415	608	758
5.6	0.023	457	665	806
5.7	0.003	477	683	851
5.75	0	477	685	852

Data: Log Δd_t Vs. $(\Delta E)^2$ 4.40 eV Peak

Time hrs.	Δd_t X 10^3 4.4	5.75	Δd_t (E) X 10^3 4.4	4.3	4.2	4.1	4.0
2.0	194	16	178	174	156	118	72
4.0	286	22	264	262	224	168	111
6.0	361	28	333	333	273	209	131

Data: Δd_t Vs. $t^{\frac{1}{2}}$ 5.0 eV Peak

Time hrs.	Δd_t X 10^3 obs'd	Δd_t 4.4	X 10^3 5.75	Sum Δd_t X 10^3 calc'd	Δd_t 5.0
1.0	162	17	125	142	20
2.0	213	24	166	190	23
3.0	266	30	209	239	27
4.0	306	36	238	274	32
5.0	353	42	276	318	35
6.0	384	45	296	341	43
7.0	416	50	317	367	49
8.0	461	55	350	405	56
9.0	485	58	367	425	60
10.0	519	61	405	466	53
11.0	523	63	399	462	61
12.0	556	68	423	491	65

TABLE VI

Specimen: 14 D
Temperature 959 ° C.

Data: Log Δd_t Vs. $(\Delta E)^2$ 5.75 eV Peak

E eV	$(\Delta E)^2$	Δd_t X 10^3 8	10	12
5.3	0.203	520	587	669
5.4	0.123	593	665	752
5.5	0.063	662	739	836
5.6	0.023	706	796	891
5.7	0.003	735	825	919
5.75	0	740	826	919

Data: Log Δd_t Vs. $(\Delta E)^2$ 4.40 eV Peak

Time hrs.	Δd_t X 10^3 4.4	5.75	Δd_t (E) X 10^3 4.4	4.3	4.2	4.1	4.0
8.0	300	30	270	269	236	171	120
10.0	348	34	314	310	267	209	141
12.0	402	38	362	359	311	235	154

Data: Log Δd_t Vs. $t^{\frac{1}{2}}$ 5.0 eV Peak

Time hrs.	Δd_t X 10^3 obs'd	Δd_t X 10^3 4.4	5.75	Sum calc'd	Δd_t X 10^3 5.0
2.0	163	20	138	158	5
4.0	230	27	197	224	6
5.0	252	32	211	243	9
6.0	285	35	235	270	15
7.0	310	39	256	295	15
8.0	341	43	276	319	22
9.0	366	46	291	337	29
10.0	388	50	309	359	29
11.0	420	53	326	379	41
12.0	449	57	343	400	49
13.0	473	61	375	436	37
14.0	501	64	387	451	50
15.0	515	67	389	456	59

TABLE VII

Specimen: 5 D 2
Temperature 1094 °C.

Data: $\text{Log}\,\Delta d_t$ Vs $(\Delta E)^2$ 5.75 eV Peak

E eV	$(\Delta E)^2$	Δd_t X 10^3 61	92	166
5.3	0.203	602	751	993
5.4	0.123	694	862	1156
5.5	0.063	785	969	1312
5.6	0.023	857	1064	1446
5.7	0.003	880	1205	1520
5.75	0	899	1210	1518

Data: $\text{Log}\,\Delta d_t$ $(\Delta E)^2$ 4.40 eV Peak

Time mins.	Δd_t X 10^3 4.4	5.75	Δd_t (E) X 10^3 4.4	4.3	4.2	4.1	4.0
61	377	9	368	351	290	208	122
92	467	11	456	432	351	257	159
166	627	15	612	587	469	339	197

Data: Δd_t Vs. $t^{\frac{1}{2}}$ 5.0 eV Peak

Time mins.	Δd_t X 10^3 obs'd	Δd_t X 10^3 4.4	5.75	Sum calc'd	Δd_t X 10^3 5.0
15	184	12	120	132	52
30	272	18	173	191	81
46	321	22	204	226	95
61	382	26	236	262	120
77	421	29	264	293	128
92	470	32	291	323	147
124	535	37	337	374	161
166	628	43	398	441	187
201	664	46	430	476	188
224	714	48	443	491	223
264	751	51	471	522	229
311	784	54	495	549	235
371	817	56	500	556	261
431	820	57	513	570	250
491	830	57	525	582	248
537	854	58	524	582	272
657	868	60	548	608	260
745	886	61	591	652	234
865	1001	62	547	609	392

Δd_s X 10^3 5.0 eV=251 avg.

TABLE VIII

Specimen: 5 C 2
Temperature 1094°C.

Data: $\text{Log}\,\Delta d_t$ Vs. $(\Delta E)^2$ 5.75 eV Peak

E eV	$(\Delta E)^2$	Δd_t X 10^3 46	77	124
5.3	0.203	518	670	859
5.4	0.123	598	769	989
5.5	0.063	672	869	1121
5.6	0.023	727	953	1222
5.7	0.003	769	996	1271
5.75	0	769	1000	1275

Data: $\text{Log}\,\Delta d_t$ Vs. $(\Delta E)^2$ 4.40 eV Peak

Time mins.	Δd_t X 10^3 4.4	5.75	Δd_t (E) X 10^3 4.4	4.3	4.2	4.1	4.0
46	325	17	312	304	247	185	106
77	420	15	403	387	318	234	133
124	544	17	522	499	408	303	175

Data: Δd_t Vs. $t^{\frac{1}{2}}$ 5.0 eV Peak

Time mins.	Δd_t X 10^3 obs'd	Δd_t X 10^3 4.4	5.75	Sum calc'd	Δd_t X 10^3 5.0
15	201	16	147	163	38
30	261	20	193	213	48
46	326	27	237	264	62
61	375	31	274	305	70
77	422	34	308	342	80
92	460	38	335	373	87
124	544	45	395	440	104
166	585	48	429	477	108
201	609	50	446	496	113
224	626	51	449	500	126
264	643	52	448	500	143
311	642	53	459	512	130
371	664	54	477	531	133
431	676	53	480	533	143
491	695	56	496	552	143
537	710	58	493	551	159
657	687	56	500	556	131
745	694	57	493	550	144

Δd_s X 10^3 5.0 eV=140 ave.

TABLE IX

Specimen: 5 C 1
Temperature 996 °C.

Data: Log Δd_t Vs. $(\Delta E)^2$ 5.75 eV Peak

E eV	$(\Delta E)^2$	Δd_t X 10^3 4	6	8
5.3	0.203	415	573	649
5.4	0.123	481	657	743
5.5	0.063	528	731	820
5.6	0.023	591	790	891
5.7	0.003	621	810	919
5.75	0	626	809	922

Data: Log Δd_t Vs. $(\Delta E)^2$ 4.40 eV Peak

Time ~~mins.~~ hrs	$\Delta d_{4.4}^{t}$ X 10^3 5.75	4.4	$\Delta d_{4.3}^{t}$ (E) X 10^3 4.2	4.1	4.0
4.0	259 19	240	237	206	155 102
6.0	381 25	356	338	282	208 132
8.0	419 29	390	375	318	237 150

Data: Δd_t Vs. $t^{\frac{1}{2}}$ 5.0 eV Peak

Time hrs.	Δd_t X 10^3 obs'd	Δd_t X 10^3 4.40	5.75	Sum calc'd	Δd_t X 10^3 5.0
2.0	164	21	142	163	1
4.0	263	32	214	246	17
6.0	363	48	278	326	37
8.0	405	53	317	370	35
26.0	613	79	483	562	51
58.0	648	84	511	595	53
72.0	662	86	522	608	54
78.0	674	88	528	616	58
94.0	690	89	534	623	67
100.0	698	88	545	633	65

d_t X 10^3 5.0 eV = 70 avg.

APPENDIX E

Diffusion Calculations

TABLE I

Data for $-\Delta F^\circ$ Vs. T°K

Specimen	Temperature °K	$2.3\Delta d_s / l_M$ (cm^{-1}) 4.40	5.0	5.75	$-\Delta F^\circ \times 10^{-3}$ (arbitrary units) 4.40	5.0	5.75
14 M	1318	64.0	7.03	161.1	36.5	30.8	39.0
14 J	1355	70.7	-	-	37.9	-	-
14 P_2	1375	58.0	11.5	141.1	37.9	33.5	40.3
14 Q	1269	64.9	10.7	154.2	35.3	30.8	37.5
5 C 1	1269	53.0	5.15	118.6	35.8	30.0	37.9
5 C 2	1367	48.5	9.83	115.5	38.4	34.1	40.7
5 D 2	1367	45.0	12.6	106.8	38.1	34.8	40.5
Haxby -							
0.01 Fe	1523	34	-	-	44.4	-	-
0.04 Fe	1523	135	-	-	44.4	-	-
0.08 Fe	1523	280	-	-	44.5	-	-
0.40 Fe	1523	800	-	-	42.9	-	-

Oxygen pressures (atmospheres):

Crystal 14 - 1
Crystal 5 - 0.21
Haxby - 0.02 (15 mm. Hg)

TABLE II

Results of the Calculation of D for Crystal 14

Specimen	Temperature °K	$-\Delta F^\circ \times 10^{-3}$ (Calc'd)		$\Delta d_s / {}^1M$ (cm^{-1})		Slope $\times 10^3$ (sec) $^{-1/2}$		D $\times 10^{10}$ cm^2/ sec.	
		4.40	5.75	4.40	5.75	4.40	5.75	4.40	5.75
14 P_2	1375	38.3	40.6	28.8	67.0	7.27	20.0	500.0	700.0
14 J	1355	37.8	40.1	29.4	69.2	7.75	15.4	545.0	392.0
14 M	1318	36.8	39.1	29.8	71.9	4.73	10.4	198.0	167.0
14 Q	1269	35.6	37.7	31.8	73.0	2.60	6.28	52.6	58.2
14 N	1255	35.1	37.3	30.4	73.6	2.85	6.70	69.2	65.1
14 D	1232	34.6	36.7	32.4	76.4	2.43	5.20	44.2	36.5
14 L	1219	34.2	36.3	31.9	76.0	1.63	4.18	20.6	23.8
14 C	1179	33.2	35.2	33.6	78.7	1.12	2.76	8.74	9.70
14 E	1115	31.6	33.5	36.8	86.8	0.446	1.14	1.16	1.36
14 B	1065	30.3	32.1	38.9	91.2	0.203	0.52	0.215	0.258

TABLE III

Results of the Calculation of D for Crystal 5

5 D 2	1367	38.1	40.5	18.1	43.7	6.12	14.6	902.0	876.0
5 C 2	1367	38.1	40.5	18.1	43.7	6.24	14.6	936.0	836.0
5 A 3	1333	37.2	39.5	19.2	47.8	5.84	13.2	729.0	595.0
5 E	1277	35.7	38.0	19.8	48.9	3.20	6.13	207.0	119.0
5 C 1	1269	35.5	37.7	19.9	47.8	3.21	6.27	205.0	135.2
5 A 2	1239	34.8	36.9	21.1	49.5	1.64	4.07	47.4	53.1
5 A 1	1213	34.1	36.2	21.4	51.0	1.40	2.90	33.6	25.5
5 H 1	1182	33.3	35.4	22.1	54.0	0.788	1.69	10.0	7.70
5 J	1182	33.3	35.4	22.1	54.0	0.912	2.13	13.4	12.2
5 B	1123	31.8	33.7	23.7	55.4	0.335	0.787	1.57	1.59
5 J	1068	30.4	32.2	25.6	60.0	0.165	0.353	0.325	0.270

TABLE IV

Results of the Calculation of D from 5.0 eV Peak

Specimen	Temperature °K	$-\Delta F^{\circ} \times 10^{-3}$ (calc'd)	$\frac{\Delta d_s}{l_M}$ (cm^{-1})	Slope ($sec^{-1/2}$)	$D \times 10^{10}$ (cm^2/sec)
14 J	1355	33.4	5.73	1.95	913.0
14 M	1318	32.0	4.76	0.84	242.0
14 Q	1269	30.1	3.59	0.33	65.9
14 N	1255	29.6	3.36	0.33	77.3
14 D	1232	28.8	3.02	0.46	178.8
5 D 2	1367	33.8	3.90	1.84	1747.0
5 G 3	1367	33.8	3.90	1.07	590.0

APPENDIX F

Estimation of Error in the Activation Energy

A. By Standard Deviation

The plot of Figure 16. is a straight line represented by:

$$y = a + bx \qquad \ldots\ldots (1)$$

if $y \equiv \log (D \times 10^{11})$

$a = \log (Do \times 10^{11})$

$b = \dfrac{-E}{2.3R}$

$x \equiv \dfrac{1}{T} \times 10^4$ See Equation (11)

The constants a and b in equation (1) may be calculated by the method of least squares (Table I); the relationship so obtained is known the regression line of y upon x.[39] The standard deviation σ_r of the scatter about this line is given by

$$\sigma_r = \sqrt{1-r^2}\sqrt{\frac{\Sigma(y - \bar{y})^2}{n - 2}}$$

where: r = correlation coefficient defined by:

$$\frac{\Sigma(x - \bar{x})(y - \bar{y})}{\sqrt{\Sigma(x - \bar{x})^2 \Sigma(y - \bar{y})^2}}$$

and $\bar{y} = \dfrac{\Sigma y}{n}$

$\bar{x} = \dfrac{\Sigma x}{n}$

n = number of pairs of observations.

Further, the standard deviations of a and b are defined by[40]:

$$\sigma_a^2 = \frac{\sigma_r^2}{n} \quad \text{and}$$

$$\sigma_b^2 = \frac{\sigma_r^2}{\Sigma(x - \bar{x})^2}$$

The correlation coefficient r was found to be -0.993. This quantity is a test of the significance of the linear relation obtained. The

TABLE I

Data for Method of Least Squares Calculation

Specimen	Log (D X 10^{+11}) 4.40	Log (D X 10^{+11}) 5.75	$\frac{1}{T}^2$ X 10^8	$\frac{1}{T}$ X 10^4	(Log D X 10^{11})($\frac{1}{T}$ X 10^4) 4.40	(Log D X 10^{11})($\frac{1}{T}$ X 10^4) 5.75
14 P_2	3.6990	3.8451	52.85	7.27	26.892	27.954
14 J	3.7364	3.5933	54.46	7.38	27.575	26.519
14 M	3.2967	3.2227	47.76	7.60	25.055	24.493
14 Q	2.7210	2.7649	62.09	7.88	21.441	21.787
14 N	2.7401	2.8136	63.52	7.97	22,636	22.424
14 D	2.6454	2.5623	65.93	8.12	21.481	20.806
14 L	3.3139	2.3766	67.24	8.20	18.964	19.488
14 C	1.9415	1.9868	71.91	8.48	16.464	16.848
14 E	1.0645	1.1335	80.46	8.97	9.549	10.167
14 B	0.3324	0.4116	88.17	9.39	3.121	3.865
n = 20	24.5909	24.7104	664.39	81.26	193.188	194.351
5 D 2	3.9552	3.9425	53.58	7.32	28.952	28.859
5 C 2	3.9713	3.9222	53.58	7.32	29.070	28.711
5 A 2	3.8627	3.7745	56.25	7.50	28.970	28.309
5 E	3.3160	3.0755	61.31	7.83	25.964	24.081
5 C 1	3.3118	3.1310	62.09	7.88	26.097	24.672
5 A 2	2.6758	2.7251	65.12	8.07	21.594	21.992
5 A 1	2.5263	2.4065	67.90	8.24	20.817	19.830
5 H 1	2.0000	1.8865	71.57	8.46	16.920	15.960
5 J	2.1271	2.0875	71.57	8.46	17.995	17.660
5 B	1.1959	1.2041	79.21	8.90	10.644	10.716
5 J	0.5119	0.4314	87.80	9.37	4.797	4.042
n = 22	29.4540	28.5868	729.98	89.35	231.820	224.832
Totals	54.0449	53.2972	1394.37	170.61	425.008	419.183
Grand Total	107.3421				844.191	

$$\Sigma(y^2) = 321.885$$

values of r are 0 for no relation at all and ± 1 for an exact linear representation; the sign of r is also the sign of slope, b.

Thus $\sigma_r = \pm 0.1225$

and $\sigma_b = \pm 30.1 \times 10^{-3}$

$\sigma_a = \pm 18.9 \times 10^{-3}$

Since $b = -1.683 \pm 30.1 \times 10^{-3}$

then $E = +4.575\ (10^4)\quad [1.683 \pm 30.1\ (10^{-3})]$

Therefore the two errors may be stated as:

a) $E = 77.0 \pm 1.4$ kcals/mole

b) $\text{Log}\ (Do \times 10^{11}) = 16.229 \pm 0.0189$

B. By Errors in Data

The basic equation used in determining E was:

$$\Delta d_t = \frac{\Delta d_s\, 2}{l_M} \left(\frac{Dt}{\pi}\right)^{\frac{1}{2}}$$

By taking the logarithm of both sides we have:

$$\text{Log}\ \Delta d_t = \log 2 + \log \Delta d_s - \log l_M + \tfrac{1}{2} \log D + \tfrac{1}{2} \log t - \log \pi$$

Differentiating this expression gives:

$$\frac{\Delta D}{D} = 2\left[\frac{\Delta(\Delta d_t)}{\Delta d_t} - \frac{\Delta(\Delta d_s)}{\Delta d_s} + \frac{\Delta l_M}{l_M} - \tfrac{1}{2}\frac{\Delta t}{t}\right]$$

The maximum estimated error in the variable D is shown in the following table.

TABLE II

Maximum Estimated Errors

Specimen	Quantity	Measured Value		% Deviation	
		4.40	5.75	4.40	5.75
14 M	Δd_t	0.547	1.242	2.9	5.5
14 P_2	Δd_s	0.687	1.642	1.7	3.6
14 P_2	l_M	0.106 in	0.106 in	2.8	2.8
14 P_2	t	60 min.	60 min.	0.9	0.9
			Sum = $\frac{\Delta D}{D}$ (%)	2(±8.3) = 16.6	2(±12.8) = 25.6

In most cases, however, the errors in both t and Δd_t would be much less than those quoted.

The maximum measured variation in the temperature was ± 10° C. which corresponds to a maximum deviation of ± 1.2% at 850° C. (Specimen 5B); this value does not include possible errors in the actual measurement of the temperature.